Available online at www.sciencedirect.com
ScienceDirect
Comput. Methods Appl. Mech. Engrg. 296 (2015) 295–326
Computer methods in applied mechanics and engineering
www.elsevier.com/locate/cma

# On some time marching schemes for the stabilized finite element approximation of the mixed wave equation

Hector Espinoza[a,b], Ramon Codina[a,*], Santiago Badia[a,c]

[a] *Universitat Politècnica de Catalunya, Jordi Girona 1-3, Edifici C1, E-08034 Barcelona, Spain*
[b] *Escuela Superior Politécnica del Litoral ESPOL, Km 30.5 vía Perimetral, EC090902, Guayaquil, Ecuador*
[c] *Centre Internacional de Mètodes Numèrics en Enginyeria, Parc Mediterrani de la Tecnologia, Esteve Terradas 5, E-08860 Castelldefels, Spain*

Received 31 December 2014; received in revised form 14 July 2015; accepted 16 July 2015
Available online 18 August 2015

**Abstract**

In this paper we analyze time marching schemes for the wave equation in mixed form. The problem is discretized in space using stabilized finite elements. On the one hand, stability and convergence analyses of the fully discrete numerical schemes are presented using different time integration schemes and appropriate functional settings. On the other hand, we use Fourier techniques (also known as von Neumann analysis) in order to analyze stability, dispersion and dissipation. Numerical convergence tests are presented for various time integration schemes, polynomial interpolations (for the spatial discretization), stabilization methods, and variational forms. To analyze the behavior of the different schemes considered, a 1D wave propagation problem is solved.
© 2015 Elsevier B.V. All rights reserved.

*MSC:* 35F46; 35L05; 35L50; 35L65; 35M13; 65J10; 65M12; 65M15; 65M60; 76M10

*Keywords:* Time marching schemes; Dispersion; Dissipation; von Neumann analysis; Fourier analysis; Mixed wave equation

## 1. Introduction

Finite difference time marching schemes are mostly used for the time integration of evolution problems because of their efficiency and ease of implementation. In the case of partial differential equations (PDEs) in space and time, even if a given finite difference scheme has some general properties regarding stability and accuracy, the precise behavior of the scheme needs to be analyzed together with the spatial discretization employed. In this paper we aim at analyzing classical first and second order schemes for the hyperbolic wave equation, with the particularity that we write it in mixed form and discretize in space using stabilized finite element (FE) methods.

For the analysis of time discretization schemes for wave propagation problems it is customary to split the total discretization error into two parts: dispersion error and dissipation error. Dispersion is the dependency of the phase

* Corresponding author. Tel.: +34 934016486.
*E-mail addresses:* hector.espinoza@upc.edu (H. Espinoza), ramon.codina@upc.edu (R. Codina), sbadia@cimne.upc.edu (S. Badia).
*URLs:* https://upc.edu/espinoza (H. Espinoza), http://codina.rmee.upc.edu/ (R. Codina), http://badia.rmee.upc.edu/ (S. Badia).

http://dx.doi.org/10.1016/j.cma.2015.07.016
0045-7825/© 2015 Elsevier B.V. All rights reserved.

velocity on the frequency and the dispersion error is the deviation of the phase velocity with respect to the expected one for a given frequency. On the other hand, dissipation error is the decrease in amplitude with respect to the expected one. In general, dispersion and dissipation errors are higher for poorly resolved frequencies, which occurs mainly for high frequencies. The wave equation we aim to analyze is non-dispersive and non-dissipative. Therefore, it would be desirable to have non-dispersive and non-dissipative discretization schemes. This sometimes cannot be achieved, thus one just aims to have low-dispersion low-dissipation schemes [1,2]. Dispersion and/or dissipation of numerical schemes can be evaluated using Fourier techniques (see [3–5]), energy methods (see [6]), or modified equation analysis (see [4,7]). Fourier analysis can be carried out for semi-discretizations or full discretizations. Dispersion/dissipation analysis methods have been used to optimize numerical schemes [3,7]. Other properties of the continuous wave equation, such as the preservation of symplecticity, some invariants or some symmetries are even more difficult to inherit for discrete schemes. This is the motivation of the so-called geometric numerical integrators, which we will not consider in this paper (see [8], for example).

Contrary to the irreducible hyperbolic wave equation, which is of second order in space and time, the mixed wave equation is of first order in space and time. We will consider the case of a single scalar unknown, which in the mixed format unfolds into two unknowns, namely, this scalar field and a vector unknown. With regard to the space approximation, the Galerkin FE discretization of this mixed wave equation requires to satisfy a compatibility condition between the spaces of the two unknowns (scalar and vector), i.e., to use so-called inf–sup compatible interpolations. Alternatively, we can consider stabilized FE methods, which provide much more flexibility when choosing the interpolation spaces [9–11]. In particular, we can consider equal interpolation for the unknowns. Stability and convergence of the stabilized FE spatial semi-discretization of the mixed wave equation has been presented in [10,11]. Stability and convergence of fully discrete schemes have also been analyzed for the convection–diffusion equation and the Stokes equations in [12–14] using spatial and temporal approximations related to those used in the present work. Note that the use of stabilized FE methods for general first order hyperbolic equations is an old topic, which can be traced back to [15] if only the advective terms are considered. However, we exploit here the particular structure of the wave equation and the functional settings that can be associated to it; this allows us to go much further in the analysis.

In this work, we analyze the stability and convergence properties for the mixed wave equation, after time semi-discretization, space semi-discretization, and full discretization, and perform their Fourier analyses. For the time discretization, we consider backward Euler (BE), Crank–Nicolson[1] (CN) and the second order backward differentiation formula (BDF2). We will see how a symplectic time integrator (CN) compares to non-symplectic time integrators (BE and BDF2). Dispersion and dissipation of discretization methods will be evaluated through numerical experiments. This consists in solving a given problem and evaluating the solution obtained [17,18,3]. We will solve a 1D wave propagation problem to show qualitatively dispersion and dissipation of the proposed numerical schemes.

The organization of the paper is as follows. In Section 2 we present the problem statement and its space–time discretization. In Section 3 we present stability and convergence results of the fully discrete problem obtained using variational techniques. We provide results for all the methods considered, even though we only present one sample of the proofs of these results. In Section 4 we present a complete Fourier analysis for the 1D wave equation in mixed form, from which precise information on the behavior of the different schemes can be drawn. Numerical results are presented in Section 5 and, finally, in Section 6 the conclusions of the work are summarized. This paper is a continuation of our work on the approximation of the mixed form of the wave equation presented in [10,11]. Frequent reference is made to these two papers, to which the reader is addressed for details.

## 2. Problem statement and numerical approximation

### 2.1. Initial and boundary value problem

The problem we consider is an initial and boundary value problem posed in a time interval $\Upsilon := (0, T)$ and in a spatial domain $\Omega \subset \mathbb{R}^d$, ($d = 1,\ 2$ or 3). Let $t \in \Upsilon$ be a given time instant in the temporal domain and $\boldsymbol{x} \in \Omega$ a given

[1] The original CN discretization scheme was devised to solve numerically PDEs of heat-conduction type; it is a space–time discretization based on finite differences. Sometimes CN is used to refer to the implicit midpoint method or the (implicit) trapezoidal rule and there is no agreement in the literature [16]. We have to mention that for linear operators (which is the case of the mixed wave equation) the trapezoidal rule and the implicit midpoint method are equivalent.

point in the spatial domain. We define the space–time domain as $\Xi := \Omega \times \Upsilon$. Let $\Gamma$ be the boundary of the domain $\Omega$. We split $\Gamma$ into three disjoint sets denoted as $\Gamma_p$, $\Gamma_u$ and $\Gamma_o$. The scalar unknown $p$ is enforced on $\Gamma_p$, the normal trace of the vector unknown $\gamma_n \boldsymbol{u}$ on $\Gamma_u$, and a simple non reflecting boundary condition (NRBC) on $\Gamma_o$. Although the boundary conditions are irrelevant for the von Neumann analysis, we just mention them for completeness.

The problem consists in finding $p : \Xi \longrightarrow \mathbb{R}$ and $\boldsymbol{u} : \Xi \longrightarrow \mathbb{R}^d$ such that

$$\mu_p \partial_t p + \nabla \cdot \boldsymbol{u} = f_p, \tag{1}$$

$$\mu_u \partial_t \boldsymbol{u} + \nabla p = \boldsymbol{f}_u, \tag{2}$$

with the following initial conditions

$$p(\boldsymbol{x}, 0) = 0, \qquad \boldsymbol{u}(\boldsymbol{x}, 0) = \boldsymbol{0}, \tag{3}$$

and with the following boundary conditions

$$p = 0 \quad \text{on } \Gamma_p, \qquad \gamma_n \boldsymbol{u} := \boldsymbol{n} \cdot \boldsymbol{u} = 0 \quad \text{on } \Gamma_u, \qquad \mu_p^{\frac{1}{2}} p = \mu_u^{\frac{1}{2}} \gamma_n \boldsymbol{u} \quad \text{on } \Gamma_o, \tag{4}$$

where $\mu_p > 0$ and $\mu_u > 0$ are physical coefficients such that $c^2 = \left(\mu_p \mu_u\right)^{-1}$, $c$ is the wave speed, $f_p$ and $\boldsymbol{f}_u$ are forcing terms, $\boldsymbol{n}$ is the unit outward normal to the boundary of the domain and $\gamma_n$ is the normal trace operator. In the previous equations and in what follows, we use the following convention: lower-case bold italic letters represent vectors in $\mathbb{R}^d$, lower-case non-bold italic letters represent scalars, whereas upper-case non-bold italic letters may be arrays or matrices.

Let $\Psi$ be a generic spatial domain, i.e. $\Omega$ or $\Gamma$ or part of them. Whenever they are well defined, we denote by $L^2(\Psi)$ the space of square integrable functions defined on $\Psi$, by $H^1(\Psi)$ the space of functions in $L^2(\Psi)$ with derivatives in $L^2(\Psi)$, by $H(\text{div}, \Psi)$ the space of vector functions with components and divergence in $L^2(\Psi)$, and by $L^2(\Psi)^d$ the space of vector functions with components in $L^2(\Psi)$. Additionally, for an arbitrary normed functional space $\mathtt{X}$, its norm will be denoted as $\|\cdot\|_{\mathtt{X}}$. In the case of $L^2(\Omega)$ or $L^2(\Omega)^d$ the $L^2$-norm will simply be denoted as $\|\cdot\|$ and the $L^2$-inner-product as $(\cdot, \cdot)$ Furthermore, the space of functions whose $\mathtt{X}$-norm is $C^r$ continuous in the time interval $\Upsilon$ will be denoted by $C^r(\Upsilon; \mathtt{X})$. We will only be interested in the cases $r = 0$ and $r = 1$. Functions whose $\mathtt{X}$-norm is $L^p$ in $\Upsilon$ will be denoted by $L^p(\Upsilon; \mathtt{X})$; when $\mathtt{X} = L^2(\Omega)$ or $\mathtt{X} = L^2(\Omega)^d$, the compact notation $L^p(L^2)$ will sometimes be used. Furthermore, let $\mathtt{V}_p$, $\mathtt{V}_u$ be spaces associated with $p$ and $\boldsymbol{u}$ respectively. These spaces will be defined afterwards because they depend on the functional setting. Additionally, let us define $\mathtt{V} := \mathtt{V}_p \times \mathtt{V}_u$ and $\mathtt{L} := L^2(\Omega) \times L^2(\Omega)^d$.

Problem (1)–(2) with appropriate initial and boundary conditions will be well-posed for:

$$p \in C^1\left(\Upsilon; L^2(\Omega)\right) \cap C^0\left(\Upsilon; \mathtt{V}_p\right), \qquad \boldsymbol{u} \in C^1\left(\Upsilon; L^2(\Omega)^d\right) \cap C^0\left(\Upsilon; \mathtt{V}_u\right),$$

with $f_p$ and $\boldsymbol{f}_u$ regular enough.

### 2.2. Variational problem

The variational form of problem (1)–(4) can be expressed in three different ways. Each one requires a certain regularity on the unknowns $p$ and $\boldsymbol{u}$. The problem reads: find $[p, \boldsymbol{u}] \in C^1(\Upsilon; \mathtt{L}) \cap C^0(\Upsilon; \mathtt{V})$ such that

$$\mathcal{B}([p, \boldsymbol{u}], [q, \boldsymbol{v}]) = \mathcal{L}([q, \boldsymbol{v}]),$$

for all test functions $[q, \boldsymbol{v}] \in \mathtt{V}$, and satisfying the initial conditions. The bilinear form $\mathcal{B}$, the linear form $\mathcal{L}$ and the space $\mathtt{V}$ are defined in three different ways depending on the variational form into consideration. For simplicity, we will assume that the forcing terms $f_p$ and $\boldsymbol{f}_u$ are square integrable, although we could relax this regularity requirement and assume they belong to the dual space of $\mathtt{V}_p$ and $\mathtt{V}_u$, respectively. Let us also define two auxiliary variables denoted as $\kappa_p$ and $\kappa_u$:

$$\kappa_p := \left(\frac{\mu_p}{\mu_u}\right)^{\frac{1}{2}}, \qquad \kappa_u := \left(\frac{\mu_u}{\mu_p}\right)^{\frac{1}{2}}.$$

The possible variational formulations of the problem are the following [10,11]:

*Variational form I.*

$$\mathtt{V}_p = \left\{ q \in H^1(\Omega) \,\middle|\, q = 0 \text{ on } \Gamma_p \right\},$$
$$\mathtt{V}_u = \left\{ \boldsymbol{v} \in H(\mathrm{div},\, \Omega) \,\middle|\, \gamma_n \boldsymbol{v} = 0 \text{ on } \Gamma_u \text{ and } \gamma_n \boldsymbol{v} \in L^2(\Gamma_\mathrm{o}) \right\}$$
$$\mathcal{B}\left([p, \boldsymbol{u}], [q, \boldsymbol{v}]\right) = \mu_p \left(\partial_t p, q\right) + \left(\nabla \cdot \boldsymbol{u}, q\right) + \mu_u \left(\partial_t \boldsymbol{u}, \boldsymbol{v}\right) + \left(\nabla p, \boldsymbol{v}\right) \tag{5}$$
$$\mathcal{L}\left([q, \boldsymbol{v}]\right) = \left(f_p, q\right) + \left(\boldsymbol{f}_u, \boldsymbol{v}\right) \tag{6}$$
$$p = 0 \quad \text{on } \Gamma_p, \text{ Strongly imposed} \tag{7}$$
$$\gamma_n \boldsymbol{u} = 0 \quad \text{on } \Gamma_u, \text{ Strongly imposed} \tag{8}$$
$$\mu_p^{\frac{1}{2}} p = \mu_u^{\frac{1}{2}} \gamma_n \boldsymbol{u} \quad \text{on } \Gamma_\mathrm{o}, \text{ Strongly imposed.} \tag{9}$$

*Variational form II.*

$$\mathtt{V}_p = L^2(\Omega), \qquad \mathtt{V}_u = \left\{ \boldsymbol{v} \in H(\mathrm{div},\, \Omega) \,\middle|\, \gamma_n \boldsymbol{v} = 0 \text{ on } \Gamma_u \text{ and } \gamma_n \boldsymbol{v} \in L^2(\Gamma_\mathrm{o}) \right\}$$
$$\mathcal{B}\left([p, \boldsymbol{u}], [q, \boldsymbol{v}]\right) = \mu_p \left(\partial_t p, q\right) + \left(\nabla \cdot \boldsymbol{u}, q\right) + \mu_u \left(\partial_t \boldsymbol{u}, \boldsymbol{v}\right) - \left(p, \nabla \cdot \boldsymbol{v}\right) + \kappa_u \int_{\Gamma_\mathrm{o}} (\gamma_n \boldsymbol{v})(\gamma_n \boldsymbol{u})\, \mathrm{d}\Gamma \tag{10}$$
$$\mathcal{L}\left([q, \boldsymbol{v}]\right) = \left(f_p, q\right) + \left(\boldsymbol{f}_u, \boldsymbol{v}\right) \tag{11}$$
$$p = 0 \quad \text{on } \Gamma_p, \text{ Weakly imposed} \tag{12}$$
$$\gamma_n \boldsymbol{u} = 0 \quad \text{on } \Gamma_u, \text{ Strongly imposed} \tag{13}$$
$$\mu_p^{\frac{1}{2}} p = \mu_u^{\frac{1}{2}} \gamma_n \boldsymbol{u} \quad \text{on } \Gamma_\mathrm{o}, \text{ Weakly imposed.} \tag{14}$$

*Variational form III.*

$$\mathtt{V}_p = \left\{ q \in H^1(\Omega) \,\middle|\, q = 0 \text{ on } \Gamma_p \right\}, \qquad \mathtt{V}_u = L^2(\Omega)^d$$
$$\mathcal{B}\left([p, \boldsymbol{u}], [q, \boldsymbol{v}]\right) = \mu_p \left(\partial_t p, q\right) - \left(\boldsymbol{u}, \nabla q\right) + \mu_u \left(\partial_t \boldsymbol{u}, \boldsymbol{v}\right) + \left(\nabla p, \boldsymbol{v}\right) + \kappa_p \int_{\Gamma_\mathrm{o}} pq\, \mathrm{d}\Gamma \tag{15}$$
$$\mathcal{L}\left([q, \boldsymbol{v}]\right) = \left(f_p, q\right) + \left(\boldsymbol{f}_u, \boldsymbol{v}\right) \tag{16}$$
$$p = 0 \quad \text{on } \Gamma_p, \text{ Strongly imposed} \tag{17}$$
$$\gamma_n \boldsymbol{u} = 0 \quad \text{on } \Gamma_u, \text{ Weakly imposed} \tag{18}$$
$$\mu_p^{\frac{1}{2}} p = \mu_u^{\frac{1}{2}} \gamma_n \boldsymbol{u} \quad \text{on } \Gamma_\mathrm{o}, \text{ Weakly imposed.} \tag{19}$$

### 2.3. Stabilized finite element formulations

Here we present two stabilized FE methods, which we will denote by the acronyms ASGS (Algebraic Sub-Grid Scales) and OSS (Orthogonal Sub-grid Scales), aimed at overcoming the instability problems of the standard Galerkin method found when the interpolating spaces do not satisfy an appropriate inf–sup condition. We focus on equal and continuous interpolations for $p$ and $\boldsymbol{u}$ and therefore, conforming FE spaces. For conciseness, we will consider quasi-uniform FE partitions $\{K\}$ of size $h$. For stabilized formulations in general non-uniform non-degenerate cases, see [19].

Let $\mathtt{V}_{p,h}$ and $\mathtt{V}_{u,h}$ be the FE spaces constructed from the FE partition $\{K\}$ to approximate $p$ and $\boldsymbol{u}$, respectively, with $\mathtt{V}_{p,h} \subset \mathtt{V}_p$ and $\mathtt{V}_{u,h} \subset \mathtt{V}_u$. Additionally, let us define $\mathtt{V}_h = \mathtt{V}_{p,h} \times \mathtt{V}_{u,h}$. Stabilized FE methods deal with the following problem: find a pair $[p_h, \boldsymbol{u}_h] \in \mathcal{C}^1(\Upsilon; \mathtt{V}_h)$ with initial conditions $p_h(\boldsymbol{x}, 0) = 0$, $\boldsymbol{u}_h(\boldsymbol{x}, 0) = \boldsymbol{0}$ such that

$$\mathcal{B}_s\left([p_h, \boldsymbol{u}_h], [q_h, \boldsymbol{v}_h]\right) = \mathcal{L}_s\left([q_h, \boldsymbol{v}_h]\right), \tag{20}$$

Table 1
Stabilization parameters order and length scales definition.

| Variational form | I | II | III |
|---|---|---|---|
| $\ell_p$ | $\ell_p = \ell_u$ | $\mathrm{L}_0^2/h$ | $h$ |
| $\ell_u$ | $\ell_p = \ell_u$ | $h$ | $\mathrm{L}_0^2/h$ |
| $\tau_p$ | $\mathcal{O}(h)$ | $\mathcal{O}(1)$ | $\mathcal{O}(h^2)$ |
| $\tau_u$ | $\mathcal{O}(h)$ | $\mathcal{O}(h^2)$ | $\mathcal{O}(1)$ |

for all test functions $[q_h, \boldsymbol{v}_h] \in \mathtt{V}_h$, where the bilinear form $\mathcal{B}_s$ and the linear form $\mathcal{L}_s$ include the Galerkin terms and additional stabilization terms. Depending on how the stabilization part is designed, a different stabilization method arises. Below, we present two methods, namely ASGS and OSS. The stabilization terms depend on the choice of the so-called stabilization parameters $\tau_p$ and $\tau_u$.

The ASGS method is an extension to the mixed form of the wave equation of the method proposed in [20,21]. It consists in solving problem (20) and taking the bilinear form $\mathcal{B}_s$ and the linear form $\mathcal{L}_s$ as:

$$\mathcal{B}_s\left([p_h, \boldsymbol{u}_h], [q_h, \boldsymbol{v}_h]\right) = \mathcal{B}\left([p_h, \boldsymbol{u}_h], [q_h, \boldsymbol{v}_h]\right) + \left(\mu_p \partial_t p_h + \nabla \cdot \boldsymbol{u}_h, \tau_p \nabla \cdot \boldsymbol{v}_h\right) + \left(\mu_u \partial_t \boldsymbol{u}_h + \nabla p_h, \tau_u \nabla q_h\right), \tag{21}$$

$$\mathcal{L}_s\left([q_h, \boldsymbol{v}_h]\right) = \mathcal{L}\left([q_h, \boldsymbol{v}_h]\right) + \left(f_p, \tau_p \nabla \cdot \boldsymbol{v}_h\right) + \left(\boldsymbol{f}_u, \tau_u \nabla q_h\right). \tag{22}$$

The OSS method is an extension to the wave equation in mixed form of the method proposed in [22,23]. It consists in solving problem (20) and taking the bilinear form $\mathcal{B}_s$ and the linear form $\mathcal{L}_s$ as:

$$\mathcal{B}_s\left([p_h, \boldsymbol{u}_h], [q_h, \boldsymbol{v}_h]\right) = \mathcal{B}\left([p_h, \boldsymbol{u}_h], [q_h, \boldsymbol{v}_h]\right) + \left(P_p{}^{\perp}\left(\nabla \cdot \boldsymbol{u}_h\right), \tau_p \nabla \cdot \boldsymbol{v}_h\right) + \left(P_u{}^{\perp}\left(\nabla p_h\right), \tau_u \nabla q_h\right), \tag{23}$$

$$\mathcal{L}_s\left([q_h, \boldsymbol{v}_h]\right) = \mathcal{L}\left([q_h, \boldsymbol{v}_h]\right) + \left(P_p{}^{\perp}\left(f_p\right), \tau_p \nabla \cdot \boldsymbol{v}_h\right) + \left(P_u{}^{\perp}\left(\boldsymbol{f}_u\right), \tau_u \nabla q_h\right), \tag{24}$$

where $P_p{}^{\perp}(\cdot) = I(\cdot) - P_p(\cdot)$ and $P_u{}^{\perp}(\cdot) = I(\cdot) - P_u(\cdot)$, $P_p(\cdot)$ being the $L^2(\Omega)$ projection on $\mathtt{V}_{p,h}$ and $P_u(\cdot)$ the $L^2(\Omega)$ projection on $\mathtt{V}_{u,h}$. This in particular implies that $P_p(\cdot) = 0$ on $\Gamma_p$ for variational forms I and III and that $\boldsymbol{n} \cdot P_u(\cdot) = 0$ on $\Gamma_u$ for variational forms I and II. Let us remark that for the sake of conciseness we will not consider in this paper the so-called dynamic subscales introduced in [23], even if we favor them and their use is crucial in the case of very small time steps (see also [24,25]).

An important ingredient of stabilized formulations are the stabilization parameters. In our case, we compute them in all formulations as:

$$\tau_p = C_\tau h \sqrt{\frac{\mu_u}{\mu_p}} \sqrt{\frac{\ell_p}{\ell_u}}, \qquad \tau_u = C_\tau h \sqrt{\frac{\mu_p}{\mu_u}} \sqrt{\frac{\ell_u}{\ell_p}}, \tag{25}$$

where $C_\tau$ is a dimensionless algorithmic constant and $\ell_p$, $\ell_u$ are length scales corresponding to $p$ and $\boldsymbol{u}$, respectively. As it was shown in the analysis presented in [10], in order to mimic at the discrete level the proper functional setting of the continuous problem the length scales $\ell_p$ and $\ell_u$ should be taken as shown in Table 1, where $\mathrm{L}_0$ is a fixed length scale of the problem that can be fixed a priori. The motivation for designing the stabilization parameters can be found in [26,9].

### 2.4. Full discretization

To discretize in time we will use standard finite difference schemes of first and second order, namely, the BE, the CN and the BDF2 schemes. Let $0 = t^0 < \cdots < t^n < \cdots t^N = T$ be a finite difference partition of $\Upsilon$ of size $\delta t$, that we take constant for the sake of simplicity. Let $U$ be the sequence of exact solutions $U := \{U^n\}_{n=0}^N := \left\{\left[p(\boldsymbol{x}, t^n), \boldsymbol{u}(\boldsymbol{x}, t^n)\right]\right\}_{n=0}^N$. We will often abbreviate $p^n := p(\boldsymbol{x}, t^n)$ and $\boldsymbol{u}^n := \boldsymbol{u}(\boldsymbol{x}, t^n)$; the same symbol will be used for a time approximation to these unknowns. Let $U_h$ be the sequence of approximate solutions of the fully discrete problem, that is $U_h := \left\{U_h^n\right\}_{n=0}^N := \left\{\left[p_h^n, \boldsymbol{u}_h^n\right]\right\}_{n=0}^N$. This fully discrete problem reads: find the sequence $U_h$ such that

$$\mathcal{B}_h\left(U_h, V_h\right) = \mathcal{L}_h\left(V_h\right), \tag{26}$$

for all $V_h$. The definitions of $\mathcal{B}_h$ and $\mathcal{L}_h$ depend on the combination of space and time discretization and will be given in the next section, where the stability and convergence properties of the fully discrete methods are presented.

To simplify notation we will use the backward ($D^r_{\mathrm{B},q,s}$) central ($D^r_{\mathrm{C},q,s}$) and forward ($D^r_{\mathrm{F},q,s}$) difference operators for the $r$th derivative, of order $q$ and in a time interval of size $s\delta t$. For instance, the BE and BDF2 approximations of the time derivative for the scalar unknown will be

$$D^1_{\mathrm{B},1,1}p^n = \frac{p^n - p^{n-1}}{\delta t}, \qquad D^1_{\mathrm{B},2,1}p^n = \frac{3p^n - 4p^{n-1} + p^{n-2}}{2\delta t}.$$

## 3. Stability and convergence results

### 3.1. Preliminaries

We present here the results of stability and convergence of the fully discrete methods arising from the combination of time marching schemes (BE, CN and BDF2) and spatial stabilized FE methods (ASGS and OSS). We provide stability and convergence results for each fully discrete method. In order to do that, we use the concept of $\Lambda$-coercivity, used for the first time in [12]. This concept is equivalent to the concept of T-coercivity [27–30] but it was coined before under the name of $\Lambda$-coercivity in [12].

The concept of $\Lambda$-coercivity aids us in the proof of stability and later in the convergence analysis. The proofs are similar to the ones shown in [10,11], but considering now the time-discretization as well. Only one of such proofs will be developed here, the others following very similar strategies.

As usual, we use $C$ for a generic constant independent of the mesh size $h$ and time step $\delta t$. The value of $C$ may be different at different occurrences. Additionally, we will use the notations $A \gtrsim B$ and $A \lesssim B$ to indicate that $A \geq CB$ and $A \leq CB$ for any $A$ and $B$ depending on the solution and the data. All our results are presented in such a way that $C$ is independent of the dimensional system, i.e., $C$ is dimensionless.

Let $U_I$ be the sequence of *projected* solutions $U_I := \left\{\left[p_I^n, \boldsymbol{u}_I^n\right]\right\}_{n=0}^N$, where $p_I^n := \Pi_p^n(p^n)$ and $\boldsymbol{u}_I^n := \Pi_u^n(\boldsymbol{u}^n)$, where $\Pi_p^n(\cdot)$ and $\Pi_u^n(\cdot)$ are adequate interpolants onto the FE spaces, taken to be projections. Notice that this notation allows us to take different interpolants at different time steps.

Let us define some auxiliary norms to ease notation in the following:

$$\left|\!\left|\!\left| V^n \right|\!\right|\!\right|_0^2 := \mu_p \left\| q^n \right\|^2 + \mu_u \left\| \boldsymbol{v}^n \right\|^2, \tag{27}$$

$$\left|\!\left|\!\left| V \right|\!\right|\!\right|_B^2 := (1+\sigma)\kappa_p \left\| q \right\|^2_{\ell^2(\Upsilon, L^2(\Gamma_{\mathrm{o}}))} + (1-\sigma)\kappa_u \left\| \gamma_n \boldsymbol{v} \right\|^2_{\ell^2(\Upsilon, L^2(\Gamma_{\mathrm{o}}))}, \tag{28}$$

$$\left|\!\left|\!\left| F \right|\!\right|\!\right|_F^2 := \frac{1}{\mu_p}\left\| f_p \right\|^2_{\ell^1(\Upsilon, L^2(\Omega))} + \frac{1}{\mu_u}\left\| \boldsymbol{f}_u \right\|^2_{\ell^1(\Upsilon, L^2(\Omega))} + \tau_p \left\| f_p \right\|^2_{\ell^2(\Upsilon, L^2(\Omega))} + \tau_u \left\| \boldsymbol{f}_u \right\|^2_{\ell^2(\Upsilon, L^2(\Omega))}, \tag{29}$$

with $\sigma = -1, 0, 1$ for variational forms I, II and III respectively, and $\|\cdot\|_{\ell^p(\Upsilon,\mathtt{X})}$ stands for the $\ell^p$-norm of a sequence of $\mathtt{X}$-norms associated to the time discretization of $\Upsilon$. When $\mathtt{X} = L^q(\Omega)$, we will use the abbreviation $\ell^p(\Upsilon, L^q(\Omega)) \equiv \ell^p(L^q)$.

For the convergence analysis we need to define three types of errors: the projection error, the discretization error, and the total error. The projection error is the error between the exact solution and the projected exact solution and is defined as $\varepsilon := \{\varepsilon^n\}_{n=0}^N := \left\{[\varepsilon_p^n, \boldsymbol{\varepsilon}_u^n]\right\}_{n=0}^N := U - U_I$. The discretization error is the error between the discrete solution and the projected exact solution and is defined as $e := \{e^n\}_{n=0}^N := \left\{[e_p^n, \boldsymbol{e}_u^n]\right\}_{n=0}^N := U_h - U_I$. Finally, the total error is the error between the exact solution and the discrete solution and is defined as $\xi := \{\xi^n\}_{n=0}^N := \left\{[\xi_p^n, \boldsymbol{\xi}_u^n]\right\}_{n=0}^N := U - U_h$.

### 3.2. Analysis strategy

As mentioned above, all the methods considered have the form (26). We have proved that all of them (ASGS and OSS for the spatial discretization, considering the three possible variational formulations, and BE, CN and BDF2 for the time integration) are stable and optimally convergent, with the convergence order in space and time that should

be expected. However, including all the proofs would be extremely long and tedious. Rather than this, we explain in what follows the analysis strategy that we have employed, give the details of the terms involved for each method in the following subsection and present then the proof of the simplest case.

For all methods we have proved $\Lambda$-coercivity, stability and convergence in an appropriate norm $|||\cdot|||$ that depends on the method. More precisely, we have shown that

1. $\Lambda$-**coercivity**. If $V$ is a sequence of functions, either continuous or discrete in space, there exists a map $\Lambda(V)$ such that
$$\mathcal{B}_h(V, \Lambda(V)) \gtrsim |||V|||^2, \qquad |||\Lambda(V)||| \lesssim |||V|||, \tag{30}$$
for all $V$. From this property one easily gets stability in the form of an inf–sup condition (see [12]).
2. **Stability**. The discrete solution $U_h$ satisfies
$$|||U_h||| \lesssim |||F|||_*, \tag{31}$$
for an appropriate norm $|||F|||_*$ of the data (the forcing terms).
3. **Convergence**. Of course, the final objective is to provide an estimate for the total error $\xi$ in some norm. We can show that if $U$ is the sequence of continuous solutions and $U_h$ the sequence of discrete solutions, then
$$|||U - U_h||| \lesssim E(h, \delta t), \tag{32}$$
for a certain error function $E(h, \delta t)$. At this point, let us remark that convergence is *not* a more or less straightforward consequence of stability, since the discrete problem is not consistent in the variational sense. To prove convergence we need to deal with the consistency error
$$\mathcal{C}(U, V_h) := \mathcal{L}_h(V_h) - \mathcal{B}_h(U, V_h). \tag{33}$$
From this definition it is easy to arrive at
$$\mathcal{B}_h(e, V_h) = \mathcal{B}_h(\varepsilon, V_h) + \mathcal{C}(U, V_h). \tag{34}$$

### 3.3. Forms, norms and error functions

Recalling that we have taken as zero the initial conditions, all methods are solely defined by the bilinear form $\mathcal{B}_h$ and the linear form $\mathcal{L}_h$. These are given for all methods in Table 2. The only comment that needs to be made is that in practice BDF2 can be started either with BE or CN. Numerical experiments show no difference in the convergence rate, even if theoretical error estimates are not optimal for convergence in terms of $\delta t$ when BDF2 is started with BE for variational forms II and III. In other words, when BE is chosen to start BDF2, some terms of the error coming from the BE part will not be of order $\delta t^2$ for variational forms II or III (e.g. the term $\delta t^2 \tau_p \left\| \mu_p \partial_{tt} p \right\|^2_{\ell^2(L^2)}$ for variational form II. See Tables 4 and 5). Obviously, we are assuming $\delta t$ proportional to $h$ to exclude variational form I from this statement.

The stability analysis of the different methods relies on the expression of map $\Lambda(V)$ satisfying (30), the norm of the unknown $|||V|||$ and the norm of the forcing terms $|||F|||_*$. These are all given in Table 3. Note that in this table use is made of abbreviations (27)–(29). The expressions of $|||F|||_*$ determine the regularity required for the data in each case.

Finally, Tables 4 and 5 provide the error functions of the error estimates (32) for the ASGS and the OSS method, respectively. There are many terms in these expressions with the same convergence order. However, including all of them gives an indication of the possible sources of error, as well as of the required regularity of the continuous solution to obtain optimal convergence rates.

### 3.4. A sample of the proofs: ASGS-BE method

As an example of how to prove (30)–(32), we present now the proof of these results for the simplest of the six methods considered, namely, ASGS for the space discretization and BE for the time integration. The proof of the rest of methods is more or less involved, but follows the same ideas.

Table 2
Forms that define the methods.

| Method | $\mathcal{B}_h$ and $\mathcal{L}_h$ |
|---|---|
| ASGS-BE | $\mathcal{B}_h\left(U_h, V_h\right) = \sum_{n=1}^{N} \delta t \left[\left(\mu_p D^1_{\mathrm{B},1,1} p_h^n + \nabla\cdot \boldsymbol{u}_h^n, q_h^n + \tau_p \nabla\cdot \boldsymbol{v}_h^n\right) + \left(\mu_u D^1_{\mathrm{B},1,1} \boldsymbol{u}_h^n + \nabla p_h^n, \boldsymbol{v}_h^n + \tau_u \nabla q_h^n\right)\right]$<br>$\mathcal{L}_h\left(V_h\right) = \sum_{n=1}^{N} \delta t \left({f_p}^n, q_h^n + \tau_p \nabla\cdot \boldsymbol{v}_h^n\right) + \sum_{n=1}^{N} \delta t \left({\boldsymbol{f}_u}^n, \boldsymbol{v}_h^n + \tau_u \nabla q_h^n\right)$ |
| ASGS-CN | $\mathcal{B}_h\left(U_h, V_h\right) = \sum_{n=1}^{N} \delta t \left[\left(\mu_p D^1_{\mathrm{B},1,1} p_h^n + \nabla\cdot {\boldsymbol{u}_h}^{n-\frac{1}{2}}, q_h^n + \tau_p \nabla\cdot \boldsymbol{v}_h^n\right)\right.$<br>$\left. + \left(\mu_u D^1_{\mathrm{B},1,1} \boldsymbol{u}_h^n + \nabla {p_h}^{n-\frac{1}{2}}, \boldsymbol{v}_h^n + \tau_u \nabla q_h^n\right)\right]$<br>$\mathcal{L}_h\left(V_h\right) = \sum_{n=1}^{N} \delta t \left({f_p}^{n-\frac{1}{2}}, q_h^n + \tau_p \nabla\cdot \boldsymbol{v}_h^n\right) + \sum_{n=1}^{N} \delta t \left({\boldsymbol{f}_u}^{n-\frac{1}{2}}, \boldsymbol{v}_h^n + \tau_u \nabla q_h^n\right)$ |
| ASGS-BDF2 | $\mathcal{B}_h\left(U_h, V_h\right) = \delta t \left[\left(\mu_p D^1_{\mathrm{B},1,1} p_h^1 + \nabla\cdot {\boldsymbol{u}_h}^{1-\frac{1}{2}}, q_h^1 + \tau_p \nabla\cdot \boldsymbol{v}_h^1\right) + \left(\mu_u D^1_{\mathrm{B},1,1} \boldsymbol{u}_h^1 + \nabla {p_h}^{1-\frac{1}{2}}, \boldsymbol{v}_h^1 + \tau_u \nabla q_h^1\right)\right]$<br>$+ \sum_{n=2}^{N} \delta t \left[\left(\mu_p D^1_{\mathrm{B},2,1} p_h^n + \nabla\cdot \boldsymbol{u}_h^n, q_h^n + \tau_p \nabla\cdot \boldsymbol{v}_h^n\right) + \left(\mu_u D^1_{\mathrm{B},2,1} \boldsymbol{u}_h^n + \nabla p_h^n, \boldsymbol{v}_h^n + \tau_u \nabla q_h^n\right)\right]$<br>$\mathcal{L}_h\left(V_h\right) = \delta t \left({f_p}^{1-\frac{1}{2}}, q_h^1 + \tau_p \nabla\cdot \boldsymbol{v}_h^1\right) + \sum_{n=2}^{N} \delta t \left({f_p}^n, q_h^n + \tau_p \nabla\cdot \boldsymbol{v}_h^n\right)$<br>$+\delta t \left({\boldsymbol{f}_u}^{1-\frac{1}{2}}, \boldsymbol{v}_h^1 + \tau_u \nabla q_h^1\right) + \sum_{n=2}^{N} \delta t \left({\boldsymbol{f}_u}^n, \boldsymbol{v}_h^n + \tau_u \nabla q_h^n\right)$ |
| OSS-BE | $\mathcal{B}_h\left(U_h, V_h\right) = \sum_{n=1}^{N} \delta t \left[\left(\mu_p D^1_{\mathrm{B},1,1} p_h^n + \nabla\cdot \boldsymbol{u}_h^n, q_h^n\right) + \tau_p \left(P_p{}^{\perp}[\nabla\cdot \boldsymbol{u}_h^n], \nabla\cdot \boldsymbol{v}_h^n\right)\right]$<br>$+ \sum_{n=1}^{N} \delta t \left[\left(\mu_u D^1_{\mathrm{B},1,1} \boldsymbol{u}_h^n + \nabla p_h^n, \boldsymbol{v}_h^n\right) + \tau_u \left(P_u{}^{\perp}[\nabla p_h^n], \nabla q_h^n\right)\right]$<br>$\mathcal{L}_h\left(V_h\right) = \sum_{n=1}^{N} \delta t \left[\left({f_p}^n, q_h^n\right) + \tau_p \left(P_p{}^{\perp}[{f_p}^n], \nabla\cdot \boldsymbol{v}_h^n\right)\right] + \sum_{n=1}^{N} \delta t \left[\left({\boldsymbol{f}_u}^n, \boldsymbol{v}_h^n\right) + \tau_u \left(P_u{}^{\perp}[{\boldsymbol{f}_u}^n], \nabla q_h^n\right)\right]$ |
| OSS-CN | $\mathcal{B}_h\left(U_h, V_h\right) = \sum_{n=1}^{N} \delta t \left[\left(\mu_p D^1_{\mathrm{B},1,1} p_h^n + \nabla\cdot {\boldsymbol{u}_h}^{n-\frac{1}{2}}, q_h^n\right) + \tau_p \left(P_p^{\perp}\left(\nabla\cdot {\boldsymbol{u}_h}^{n-\frac{1}{2}}\right), \nabla\cdot \boldsymbol{v}_h^n\right)\right]$<br>$+ \sum_{n=1}^{N} \delta t \left[\left(\mu_u D^1_{\mathrm{B},1,1} \boldsymbol{u}_h^n + \nabla {p_h}^{n-\frac{1}{2}}, \boldsymbol{v}_h^n\right) + \tau_u \left(P_u^{\perp}\left(\nabla {p_h}^{n-\frac{1}{2}}\right), \nabla q_h^n\right)\right]$<br>$\mathcal{L}_h\left(V_h\right) = \sum_{n=1}^{N} \delta t \left[\left({f_p}^{n-\frac{1}{2}}, q_h^n\right) + \tau_p \left(P_p{}^{\perp}[{f_p}^{n-\frac{1}{2}}], \nabla\cdot \boldsymbol{v}_h^n\right)\right]$<br>$+ \sum_{n=1}^{N} \delta t \left[\left({\boldsymbol{f}_u}^{n-\frac{1}{2}}, \boldsymbol{v}_h^n\right) + \tau_u \left(P_u{}^{\perp}[{\boldsymbol{f}_u}^{n-\frac{1}{2}}], \nabla q_h^n\right)\right]$ |
| OSS-BDF2 | $\mathcal{B}_h\left(U_h, V_h\right) = \delta t \left[\left(\mu_p D^1_{\mathrm{B},1,1} p_h^1 + \nabla\cdot \boldsymbol{u}_h^{\frac{1}{2}}, q_h^1 + \tau_p \nabla\cdot \boldsymbol{v}_h^1\right) + \left(P_p^{\perp}\left(\nabla\cdot \boldsymbol{u}_h^{\frac{1}{2}}\right), \tau_p \nabla\cdot \boldsymbol{v}_h^1\right)\right]$<br>$+ \sum_{n=2}^{N} \delta t \left[\left(\mu_p D^1_{\mathrm{B},2,1} p_h^n + \nabla\cdot \boldsymbol{u}_h^n, q_h^n\right) + \tau_p \left(P_p{}^{\perp}[\nabla\cdot \boldsymbol{u}_h^n], \nabla\cdot \boldsymbol{v}_h^n\right)\right]$<br>$+\delta t \left[\left(\mu_u D^1_{\mathrm{B},1,1} \boldsymbol{u}_h^1 + \nabla p_h^{\frac{1}{2}}, \boldsymbol{v}_h^1\right) + \left(P_u^{\perp}\left(\nabla p_h^{\frac{1}{2}}\right), \tau_u \nabla q_h^1\right)\right]$<br>$+ \sum_{n=2}^{N} \delta t \left[\left(\mu_u D^1_{\mathrm{B},2,1} \boldsymbol{u}_h^n + \nabla p_h^n, \boldsymbol{v}_h^n\right) + \tau_u \left(P_u{}^{\perp}[\nabla p_h^n], \nabla q_h^n\right)\right]$<br>$\mathcal{L}_h\left(V_h\right) = \delta t \left[\left({f_p}^{\frac{1}{2}}, q_h^1\right) + \tau_p \left(P_p{}^{\perp}[{f_p}^{\frac{1}{2}}], \nabla\cdot \boldsymbol{v}_h^1\right)\right] + \delta t \left[\left({\boldsymbol{f}_u}^{\frac{1}{2}}, \boldsymbol{v}_h^1\right) + \tau_u \left(P_u{}^{\perp}[{\boldsymbol{f}_u}^{\frac{1}{2}}], \nabla q_h^1\right)\right]$<br>$+ \sum_{n=2}^{N} \delta t \left[\left({f_p}^n, q_h^n\right) + \tau_p \left(P_p{}^{\perp}[{f_p}^n], \nabla\cdot \boldsymbol{v}_h^n\right)\right] + \sum_{n=2}^{N} \delta t \left[\left({\boldsymbol{f}_u}^n, \boldsymbol{v}_h^n\right) + \tau_u \left(P_u{}^{\perp}[{\boldsymbol{f}_u}^n], \nabla q_h^n\right)\right]$ |

### 3.4.1. *Proof of $\Lambda$-coercivity (30)*

From the definition of $\mathcal{B}_h$ in Table 2 and of $\Lambda(V)$ in Table 3 for the ASGS-BE method we get

$$
\begin{aligned}
\mathcal{B}_h\left(V, \Lambda\left(V\right)\right) = & \sum_{n=1}^{N} \delta t \left(\mu_p D^1_{\mathrm{B},1,1} q^n, q^n\right) + \sum_{n=1}^{N} \delta t \left(\mu_u D^1_{\mathrm{B},1,1} \boldsymbol{v}^n, \boldsymbol{v}^n\right) \\
& + \tau_p \tau_u \mu_u \sum_{n=1}^{N} \delta t \left(\nabla\cdot \boldsymbol{v}^n, \nabla\cdot \left(D^1_{\mathrm{B},1,1} \boldsymbol{v}^n\right)\right) + \tau_p \tau_u \mu_p \sum_{n=1}^{N} \delta t \left(\nabla q^n, \nabla \left(D^1_{\mathrm{B},1,1} q^n\right)\right) \\
& + \sum_{n=1}^{N} \delta t \left[\left(\nabla\cdot \boldsymbol{v}^n, q^n\right) + \left(\nabla q^n, \boldsymbol{v}^n\right)\right]
\end{aligned}
$$

Table 3
Functions to obtain $\Lambda$-coercivity and norms.

| Method | $\Lambda(V)$, $\|\|V\|\|$ and $\|\|F\|\|_*$ |
|---|---|
| ASGS-BE | $\Lambda(V) := V + \left\{[0,\boldsymbol{0}], \left\{\left[\tau_p\mu_p D^1_{\mathrm{B},1,1}q^n, \tau_u\mu_u D^1_{\mathrm{B},1,1}\boldsymbol{v}^n\right]\right\}_{n=1}^N\right\}$<br>$\|\|V\|\|^2 := \left\|\left\|V^N\right\|\right\|_0^2 + \|\|V\|\|_B^2 + \tau_p\left\|\mu_p D^1_{\mathrm{B},1,1}q^n + \nabla\cdot\boldsymbol{v}^n\right\|^2_{\ell^2(\Upsilon,L^2(\Omega))} + \tau_u\left\|\mu_u D^1_{\mathrm{B},1,1}\boldsymbol{v}^n + \nabla q^n\right\|^2_{\ell^2(\Upsilon,L^2(\Omega))}$<br>$\|\|F\|\|_*^2 := \|\|F\|\|_F^2 + \tau_p\tau_u\mu_u\left\|D^1_{\mathrm{B},1,1}f_p\right\|^2_{\ell^1(\Upsilon,L^2(\Omega))} + \tau_p\tau_u\mu_p\left\|D^1_{\mathrm{B},1,1}\boldsymbol{f}_u\right\|^2_{\ell^1(\Upsilon,L^2(\Omega))}$<br>$+\tau_p\tau_u\mu_u\left\|f_p\right\|^2_{\ell^\infty(\Upsilon,L^2(\Omega))} + \tau_p\tau_u\mu_p\left\|\boldsymbol{f}_u\right\|^2_{\ell^\infty(\Upsilon,L^2(\Omega))}$ |
| ASGS-CN | $\Lambda(V) := \left\{\left[p^0,\boldsymbol{u}^0\right], \left\{\left[p^{n-\frac12},\boldsymbol{u}^{n-\frac12}\right]\right\}_{n=1}^N\right\} + \left\{[0,\boldsymbol{0}], \left\{\left[\tau_p\mu_p D^1_{\mathrm{B},1,1}q^n, \tau_u\mu_u D^1_{\mathrm{B},1,1}\boldsymbol{v}^n\right]\right\}_{n=1}^N\right\}$<br>$\|\|V\|\|^2 := \left\|\left\|V^N\right\|\right\|_0^2 + \|\|V\|\|_B^2 + \tau_p\left\|\mu_p D^1_{\mathrm{B},1,1}q^n + \nabla\cdot\boldsymbol{v}^{n-\frac12}\right\|^2_{\ell^2(\Upsilon,L^2(\Omega))}$<br>$+\tau_u\left\|\mu_u D^1_{\mathrm{B},1,1}\boldsymbol{v}^n + \nabla q^{n-\frac12}\right\|^2_{\ell^2(\Upsilon,L^2(\Omega))}$<br>$\|\|F\|\|_*^2 := \|\|F\|\|_F^2 + \tau_p\tau_u\mu_u\left\|D^1_{\mathrm{B},1,1}f_p\right\|^2_{\ell^1(\Upsilon,L^2(\Omega))} + \tau_p\tau_u\mu_p\left\|D^1_{\mathrm{B},1,1}\boldsymbol{f}_u\right\|^2_{\ell^1(\Upsilon,L^2(\Omega))}$<br>$+\tau_p\tau_u\mu_u\left\|f_p\right\|^2_{\ell^\infty(\Upsilon,L^2(\Omega))} + \tau_p\tau_u\mu_p\left\|\boldsymbol{f}_u\right\|^2_{\ell^\infty(\Upsilon,L^2(\Omega))}$ |
| ASGS-BDF2 | $\Lambda(V) := \left\{V^0, V^{\frac12}, \{V^n\}_{n=2}^N\right\}$<br>$+\left\{[0,\boldsymbol{0}], \left[\tau_p\mu_p D^1_{\mathrm{B},1,1}q^1, \tau_u\mu_u D^1_{\mathrm{B},1,1}\boldsymbol{v}^1\right], \left\{\left[\tau_p\mu_p D^1_{\mathrm{B},2,1}q^n, \tau_u\mu_u D^1_{\mathrm{B},2,1}\boldsymbol{v}^n\right]\right\}_{n=2}^N\right\}$<br>$\|\|V\|\|^2 := \left\|\left\|V^N\right\|\right\|_0^2 + \|\|V\|\|_B^2 + \tau_p\left\|\mu_p D^1_{\mathrm{B},1,1}q^1 + \nabla\cdot\boldsymbol{v}^{\frac12}\right\|^2\delta t + \tau_u\left\|\mu_u D^1_{\mathrm{B},1,1}\boldsymbol{v}^1 + \nabla q^{\frac12}\right\|^2\delta t$<br>$+\tau_p\left\|\mu_p D^1_{\mathrm{B},2,1}q^n + \nabla\cdot\boldsymbol{v}^n\right\|^2_{\ell^2(\Upsilon,L^2(\Omega))} + \tau_u\left\|\mu_u D^1_{\mathrm{B},2,1}\boldsymbol{v}^n + \nabla q^n\right\|^2_{\ell^2(\Upsilon,L^2(\Omega))}$<br>$\|\|F\|\|_*^2 := \|\|F\|\|_F^2 + \tau_p\tau_u\mu_u\left\|D^1_{\mathrm{B},1,1}f_p{}^1\right\|^2\delta t^2 + \tau_p\tau_u\mu_u\left\|D^1_{\mathrm{B},2,1}f_p\right\|^2_{\ell^1(\Upsilon,L^2(\Omega))} + \tau_p\tau_u\mu_u\left\|f_p\right\|^2_{\ell^\infty(\Upsilon,L^2(\Omega))}$<br>$+\tau_p\tau_u\mu_p\left\|D^1_{\mathrm{B},1,1}\boldsymbol{f}_u{}^1\right\|^2\delta t^2 + \tau_p\tau_u\mu_p\left\|D^1_{\mathrm{B},2,1}\boldsymbol{f}_u\right\|^2_{\ell^1(\Upsilon,L^2(\Omega))} + \tau_p\tau_u\mu_p\left\|\boldsymbol{f}_u\right\|^2_{\ell^\infty(\Upsilon,L^2(\Omega))}$ |
| OSS-BE | $\Lambda(V) := V + \beta\Lambda_b(V) \quad (\beta \text{ small enough})$<br>$\Lambda_b(V) := \left\{[0,\boldsymbol{0}], \left\{\left[\tau_p\left(\mu_p D^1_{\mathrm{B},1,1}q^n + P_p[\nabla\cdot\boldsymbol{v}^n]\right), \tau_u\left(\mu_u D^1_{\mathrm{B},1,1}\boldsymbol{v}^n + P_u[\nabla q^n]\right)\right]\right\}_{n=1}^N\right\}$<br>$\|\|V\|\|^2 := \left\|\left\|V^N\right\|\right\|_0^2 + \|\|V\|\|_B^2 + \tau_p\left\|\mu_p D^1_{\mathrm{B},1,1}q^n + \nabla\cdot\boldsymbol{v}^n\right\|^2_{\ell^2(\Upsilon,L^2(\Omega))} + \tau_u\left\|\mu_u D^1_{\mathrm{B},1,1}\boldsymbol{v}^n + \nabla q^n\right\|^2_{\ell^2(\Upsilon,L^2(\Omega))}$<br>$\|\|F\|\|_*^2 := \|\|F\|\|_F^2$ |
| OSS-CN | $\Lambda(V) := \Lambda_a(V) + \beta\Lambda_b(V) \quad (\beta \text{ small enough})$<br>$\Lambda_a(V) := \left\{\left[p^0,\boldsymbol{u}^0\right], \left\{\left[p^{n-\frac12},\boldsymbol{u}^{n-\frac12}\right]\right\}_{n=1}^N\right\}$<br>$\Lambda_b(V) := \left\{[0,\boldsymbol{0}], \left\{\left[\tau_p\left(\mu_p D^1_{\mathrm{B},1,1}q^n + P_p[\nabla\cdot\boldsymbol{v}^{n-\frac12}]\right), \tau_u\left(\mu_u D^1_{\mathrm{B},1,1}\boldsymbol{v}^n + P_u[\nabla q^{n-\frac12}]\right)\right]\right\}_{n=1}^N\right\}$<br>$\|\|V\|\|^2 := \left\|\left\|V^N\right\|\right\|_0^2 + \|\|V\|\|_B^2 + \tau_p\left\|\mu_p D^1_{\mathrm{B},1,1}q^n + \nabla\cdot\boldsymbol{v}^{n-\frac12}\right\|^2_{\ell^2(\Upsilon,L^2(\Omega))}$<br>$+\tau_u\left\|\mu_u D^1_{\mathrm{B},1,1}\boldsymbol{v}^n + \nabla q^{n-\frac12}\right\|^2_{\ell^2(\Upsilon,L^2(\Omega))}$<br>$\|\|F\|\|_*^2 := \|\|F\|\|_F^2$ |

(*continued on next page*)

$$+\sum_{n=1}^N \delta t\,\tau_p\left\|\mu_p D^1_{\mathrm{B},1,1}q^n + \nabla\cdot\boldsymbol{v}^n\right\|^2 + \sum_{n=1}^N \delta t\,\tau_u\left\|\mu_u D^1_{\mathrm{B},1,1}\boldsymbol{v}^n + \nabla q^n\right\|^2$$

$$+\tau_p\tau_u\mu_p\mu_u\sum_{n=1}^N \delta t\left[\left(D^1_{\mathrm{B},1,1}q^n, \nabla\cdot\left(D^1_{\mathrm{B},1,1}\boldsymbol{v}^n\right)\right) + \left(D^1_{\mathrm{B},1,1}\boldsymbol{v}^n, \nabla\left(D^1_{\mathrm{B},1,1}q^n\right)\right)\right]. \tag{35}$$

Table 3 (*continued*)

| Method | $\Lambda(V)$, $\|\|\|V\|\|\|$ and $\|\|\|F\|\|\|_*$ |
|---|---|
| OSS-BDF2 | $\Lambda(V) := \Lambda_a(V) + \beta\Lambda_b(V) \quad (\beta > 0 \text{ small enough})$ |
| | $\Lambda_a(V) := \left\{ V^0, V^{\frac{1}{2}}, \{V^n\}_{n=2}^N \right\}$ |
| | $\Lambda_b(V) := \left\{ [0, \boldsymbol{0}], \left[ \tau_p \left( \mu_p D^1_{\mathrm{B},1,1} q^1 + P_p[\nabla \cdot \boldsymbol{v}^{\frac{1}{2}}] \right), \tau_u \left( \mu_u D^1_{\mathrm{B},1,1} \boldsymbol{v}^1 + P_u[\nabla q^{\frac{1}{2}}] \right) \right] \right.$ |
| | $\left. \left\{ \left[ \tau_p \left( \mu_p D^1_{\mathrm{B},2,1} q^n + P_p[\nabla \cdot \boldsymbol{v}^n] \right), \tau_u \left( \mu_u D^1_{\mathrm{B},2,1} \boldsymbol{v}^n + P_u[\nabla q^n] \right) \right] \right\}_{n=2}^N \right\}$ |
| | $\|\|\|V\|\|\|^2 := \left\| V^N \right\|_0^2 + \|\|\|V\|\|\|_B^2 + \tau_p \left\| \mu_p D^1_{\mathrm{B},1,1} q^1 + \nabla \cdot \boldsymbol{v}^{\frac{1}{2}} \right\|^2 \delta t + \tau_u \left\| \mu_u D^1_{\mathrm{B},1,1} \boldsymbol{v}^1 + \nabla q^{\frac{1}{2}} \right\|^2 \delta t$ |
| | $+\tau_p \left\| \mu_p D^1_{\mathrm{B},2,1} q^n + \nabla \cdot \boldsymbol{v}^n \right\|^2_{\ell^2(\Upsilon, L^2(\Omega))} + \tau_u \left\| \mu_u D^1_{\mathrm{B},2,1} \boldsymbol{v}^n + \nabla q^n \right\|^2_{\ell^2(\Upsilon, L^2(\Omega))}$ |
| | $\|\|\|F\|\|\|_*^2 := \|\|\|F\|\|\|_F^2$ |

Now we show how each term is bounded. The first four terms of (35) can be bounded considering zero initial conditions (3), the fact that $\tau_p \tau_u = C_\tau^2 h^2$ by (25) and the definition of $\left\| V^N \right\|_0^2$ in (27) as

$$\sum_{n=1}^N \delta t \left( \mu_p D^1_{\mathrm{B},1,1} q^n, q^n \right) + \sum_{n=1}^N \delta t \left( \mu_u D^1_{\mathrm{B},1,1} \boldsymbol{v}^n, \boldsymbol{v}^n \right) + \tau_p \tau_u \mu_u \sum_{n=1}^N \delta t \left( \nabla \cdot \boldsymbol{v}^n, \nabla \cdot \left( D^1_{\mathrm{B},1,1} \boldsymbol{v}^n \right) \right) + \tau_p \tau_u \mu_p \sum_{n=1}^N \delta t \left( \nabla q^n, \nabla \left( D^1_{\mathrm{B},1,1} q^n \right) \right) \gtrsim \left\| V^N \right\|_0^2 . \tag{36}$$

The 5th term is bounded using the divergence theorem, splitting the boundary integral into its parts $\Gamma_p$ $\Gamma_u$ $\Gamma_o$, using the boundary conditions (4) and the definition of $\|\|\|V\|\|\|_B^2$ in (28) as

$$\sum_{n=1}^N \delta t \left[ \left( \nabla \cdot \boldsymbol{v}^n, q^n \right) + \left( \nabla q^n, \boldsymbol{v}^n \right) \right] \geq \|\|\|V\|\|\|_B^2 . \tag{37}$$

The 6th and 7th terms are already what we need. The 8th and 9th terms are greater than zero by boundary conditions. Combining (35)–(37) the proof is completed.

### 3.4.2. *Proof of stability (31)*

Recalling the $\Lambda$-coercivity result we can write

$$\|\|\|U_h\|\|\|^2 \lesssim \mathcal{B}_h(U_h, \Lambda(U_h)) = \mathcal{L}_h(\Lambda(U_h)), \tag{38}$$

and using the definition of $\mathcal{L}_h$ we can write

$$\|\|\|U_h\|\|\|^2 \lesssim \sum_{n=1}^N \delta t \left( {f_p}^n, p_h^n + \tau_p \left( \mu_p D^1_{\mathrm{B},1,1} p_h^n + \nabla \cdot \boldsymbol{u}_h^n \right) \right) + \sum_{n=1}^N \delta t \left( {f_p}^n, \tau_p \nabla \cdot \tau_u \mu_u D^1_{\mathrm{B},1,1} \boldsymbol{u}_h^n \right) + \sum_{n=1}^N \delta t \left( {\boldsymbol{f}_u}^n, \boldsymbol{u}_h^n + \tau_u \left( \mu_u D^1_{\mathrm{B},1,1} \boldsymbol{u}_h^n + \nabla p_h^n \right) \right) + \sum_{n=1}^N \delta t \left( {\boldsymbol{f}_u}^n, \tau_u \nabla \tau_p \mu_p D^1_{\mathrm{B},1,1} p_h^n \right) . \tag{39}$$

The 1st and 3rd terms can be bounded as

$$\sum_{n=1}^N \delta t \left( {f_p}^n, p_h^n + \tau_p \left( \mu_p D^1_{\mathrm{B},1,1} p_h^n + \nabla \cdot \boldsymbol{u}_h^n \right) \right) + \sum_{n=1}^N \delta t \left( {\boldsymbol{f}_u}^n, \boldsymbol{u}_h^n + \tau_u \left( \mu_u D^1_{\mathrm{B},1,1} \boldsymbol{u}_h^n + \nabla p_h^n \right) \right) \lesssim \alpha_1 \|\|\|F\|\|\|_F^2 + \frac{1}{\alpha_1} \|\|\|U_h\|\|\|^2 , \tag{40}$$

Table 4
Error functions I: ASGS formulation.

| Method | $E(h,\delta t)$ |
|---|---|
| BE | $E^2(h,\delta t) \coloneqq \mu_p \left\|\varepsilon_p\right\|^2_{\ell^\infty(L^2)} + \mu_u \left\|\boldsymbol{\varepsilon}_u\right\|^2_{\ell^\infty(L^2)} + \tau_p\tau_u\mu_u \left\|\nabla\cdot\boldsymbol{\varepsilon}_u\right\|^2_{\ell^\infty(L^2)} + \tau_p\tau_u\mu_p \left\|\nabla\varepsilon_p\right\|^2_{\ell^\infty(L^2)}$ $+\frac{1}{\tau_u}\left\|\boldsymbol{\varepsilon}_u\right\|^2_{\ell^2(L^2)} + \tau_p\left\|\mu_p D^1_{\mathrm{B},1,1}\varepsilon_p\right\|^2_{\ell^2(L^2)} + \tau_p\left\|\nabla\cdot\boldsymbol{\varepsilon}_u\right\|^2_{\ell^2(L^2)} + (1+\sigma)\kappa_p\left\|\varepsilon_p\right\|^2_{\ell^2(\Upsilon,L^2(\Gamma_\mathrm{o}))}$ $+\frac{1}{\tau_p}\left\|\varepsilon_p\right\|^2_{\ell^2(L^2)} + \tau_u\left\|\mu_u D^1_{\mathrm{B},1,1}\boldsymbol{\varepsilon}_u\right\|^2_{\ell^2(L^2)} + \tau_u\left\|\nabla\varepsilon_p\right\|^2_{\ell^2(L^2)} + (1-\sigma)\kappa_u\left\|\boldsymbol{\varepsilon}_u\right\|^2_{\ell^2(\Upsilon,L^2(\Gamma_\mathrm{o}))}$ $+\tau_p\tau_u\mu_u\left\|\mu_p D^1_{\mathrm{B},1,1}\varepsilon_p\right\|^2_{\ell^\infty(L^2)} + \tau_p\tau_u\mu_u\left\|\mu_p D^2_{\mathrm{C},2,1}\varepsilon_p\right\|^2_{\ell^1(L^2)} + \tau_p\tau_u\mu_u\left\|\nabla\cdot D^1_{\mathrm{B},1,1}\boldsymbol{\varepsilon}_u\right\|^2_{\ell^1(L^2)}$ $+\tau_p\tau_u\mu_p\left\|\mu_u D^1_{\mathrm{B},1,1}\boldsymbol{\varepsilon}_u\right\|^2_{\ell^\infty(L^2)} + \tau_p\tau_u\mu_p\left\|\mu_u D^2_{\mathrm{C},2,1}\boldsymbol{\varepsilon}_u\right\|^2_{\ell^1(L^2)} + \tau_p\tau_u\mu_p\left\|\nabla D^1_{\mathrm{B},1,1}\varepsilon_p\right\|^2_{\ell^1(L^2)}$ $+\frac{\delta t^2}{\mu_p}\left\|\mu_p\partial_{tt}p\right\|^2_{\ell^1(L^2)} + \delta t^2\tau_p\left\|\mu_p\partial_{tt}p\right\|^2_{\ell^2(L^2)} + \tau_p\tau_u\mu_u\delta t^2\left(\left\|\mu_p\partial_{tt}p\right\|^2_{\ell^\infty(L^2)} + \left\|\mu_p\partial_{ttt}p\right\|^2_{\ell^1(L^2)}\right)$ $+\frac{\delta t^2}{\mu_u}\left\|\mu_u\partial_{tt}\boldsymbol{u}\right\|^2_{\ell^1(L^2)} + \delta t^2\tau_u\left\|\mu_u\partial_{tt}\boldsymbol{u}\right\|^2_{\ell^2(L^2)} + \tau_p\tau_u\mu_p\delta t^2\left(\left\|\mu_u\partial_{tt}\boldsymbol{u}\right\|^2_{\ell^\infty(L^2)} + \left\|\mu_u\partial_{ttt}\boldsymbol{u}\right\|^2_{\ell^1(L^2)}\right)$ |
| CN | $E^2(h,\delta t) \coloneqq \mu_p\left\|\varepsilon_p\right\|^2_{\ell^\infty(\Upsilon,L^2(\Omega))} + \mu_u\left\|\boldsymbol{\varepsilon}_u\right\|^2_{\ell^\infty(\Upsilon,L^2(\Omega))} + (1+\sigma)\kappa_p\left\|\varepsilon_p\right\|^2_{\ell^2(\Upsilon,L^2(\Gamma_\mathrm{o}))} + (1-\sigma)\kappa_u\left\|\boldsymbol{\varepsilon}_u\right\|^2_{\ell^2(\Upsilon,L^2(\Gamma_\mathrm{o}))}$ $+\frac{1}{\tau_u}\left\|\boldsymbol{\varepsilon}_u\right\|^2_{\ell^2(L^2)} + \tau_p\left\|\mu_p D^1_{\mathrm{B},1,1}\varepsilon_p\right\|^2_{\ell^2(L^2)} + \tau_p\left\|\nabla\cdot\boldsymbol{\varepsilon}_u\right\|^2_{\ell^2(L^2)} + \tau_p\tau_u\mu_u\left\|\nabla\cdot D^1_{\mathrm{B},1,1}\boldsymbol{\varepsilon}_u\right\|^2_{\ell^1(L^2)}$ $+\frac{1}{\tau_p}\left\|\varepsilon_p\right\|^2_{\ell^2(L^2)} + \tau_u\left\|\mu_u D^1_{\mathrm{B},1,1}\boldsymbol{\varepsilon}_u\right\|^2_{\ell^2(L^2)} + \tau_u\left\|\nabla\varepsilon_p\right\|^2_{\ell^2(L^2)} + \tau_p\tau_u\mu_p\left\|\nabla D^1_{\mathrm{B},1,1}\varepsilon_p\right\|^2_{\ell^1(L^2)}$ $+\tau_p\tau_u\mu_u\left\|\mu_p D^1_{\mathrm{B},1,1}\varepsilon_p\right\|^2_{\ell^\infty(L^2)} + \tau_p\tau_u\mu_u\left\|\mu_p D^2_{\mathrm{C},2,1}\varepsilon_p\right\|^2_{\ell^1(L^2)}$ $+\tau_p\tau_u\mu_p\left\|\mu_u D^1_{\mathrm{B},1,1}\boldsymbol{\varepsilon}_u\right\|^2_{\ell^\infty(L^2)} + \tau_p\tau_u\mu_p\left\|\mu_u D^2_{\mathrm{C},2,1}\boldsymbol{\varepsilon}_u\right\|^2_{\ell^1(L^2)}$ $+\frac{\delta t^4}{\mu_p}\left\|\mu_p\partial_{ttt}p\right\|^2_{\ell^1(L^2)} + \delta t^4\tau_p\left\|\mu_p\partial_{ttt}p\right\|^2_{\ell^2(L^2)} + \tau_p\tau_u\mu_u\delta t^4\left[\left\|\mu_p\partial_{ttt}p\right\|^2_{\ell^\infty(L^2)} + \left\|\mu_p\partial_{tttt}p\right\|^2_{\ell^1(L^2)}\right]$ $+\frac{\delta t^4}{\mu_u}\left\|\mu_u\partial_{ttt}\boldsymbol{u}\right\|^2_{\ell^1(L^2)} + \delta t^4\tau_u\left\|\mu_u\partial_{ttt}\boldsymbol{u}\right\|^2_{\ell^2(L^2)} + \tau_p\tau_u\mu_p\delta t^4\left[\left\|\mu_u\partial_{ttt}\boldsymbol{u}\right\|^2_{\ell^\infty(L^2)} + \left\|\mu_u\partial_{tttt}\boldsymbol{u}\right\|^2_{\ell^1(L^2)}\right]$ |
| BDF2 | $E^2(h,\delta t) \coloneqq \mu_p\left\|\varepsilon_p\right\|^2_{\ell^\infty(L^2)} + \mu_u\left\|\boldsymbol{\varepsilon}_u\right\|^2_{\ell^\infty(L^2)} + (1+\sigma)\kappa_p\left\|\varepsilon_p\right\|^2_{\ell^2(\Upsilon,L^2(\Gamma_\mathrm{o}))} + (1-\sigma)\kappa_u\left\|\boldsymbol{\varepsilon}_u\right\|^2_{\ell^2(\Upsilon,L^2(\Gamma_\mathrm{o}))}$ $+\frac{1}{\tau_u}\left\|\boldsymbol{\varepsilon}_u\right\|^2_{\ell^2(\Upsilon,L^2(\Omega))} + \tau_p\left\|\mu_p D^1_{\mathrm{B},1,1}\varepsilon^1_p\right\|^2\delta t + \tau_p\left\|\mu_p D^1_{\mathrm{B},2,1}\varepsilon_p\right\|^2_{\ell^2(L^2)} + \tau_p\left\|\nabla\cdot\boldsymbol{\varepsilon}_u\right\|^2_{\ell^2(L^2)}$ $+\frac{1}{\tau_p}\left\|\varepsilon_p\right\|^2_{\ell^2(L^2)} + \tau_u\left\|\mu_u D^1_{\mathrm{B},1,1}\boldsymbol{\varepsilon}^1_u\right\|^2\delta t + \tau_u\left\|\mu_u D^1_{\mathrm{B},2,1}\boldsymbol{\varepsilon}_u\right\|^2_{\ell^2(L^2)} + \tau_u\left\|\nabla\varepsilon_p\right\|^2_{\ell^2(\Upsilon,L^2(\Omega))}$ $+\tau_p\tau_u\mu_u\left\|\mu_p D^2_{\mathrm{C},2,\frac{1}{2}}\varepsilon_p^{\frac{1}{2}}\right\|^2\delta t^2 + \tau_p\tau_u\mu_p\left\|\mu_u D^2_{\mathrm{C},2,\frac{1}{2}}\boldsymbol{\varepsilon}_u^{\frac{1}{2}}\right\|^2\delta t^2$ $+\tau_p\tau_u\mu_u\left(\left\|\mu_p D^1_{\mathrm{B},2,1}\varepsilon^2_p\right\|^2 + \left\|\mu_p\left(D^1_{\mathrm{B},2,1}\varepsilon^3_p - 4D^1_{\mathrm{B},2,1}\varepsilon^2_p\right)\right\|^2\right)$ $+\tau_p\tau_u\mu_p\left(\left\|\mu_u D^1_{\mathrm{B},2,1}\boldsymbol{\varepsilon}^2_u\right\|^2 + \left\|\mu_u\left(D^1_{\mathrm{B},2,1}\boldsymbol{\varepsilon}^3_u - 4D^1_{\mathrm{B},2,1}\boldsymbol{\varepsilon}^2_u\right)\right\|^2\right)$ $+\tau_p\tau_u\mu_u\left\|\mu_p(3D^2_{\mathrm{C},4,1} - 2D^2_{\mathrm{C},2,2})\varepsilon^n_p\right\|^2_{\ell^1(L^2)} + \tau_p\tau_u\mu_p\left\|\mu_u(3D^2_{\mathrm{C},4,1} - 2D^2_{\mathrm{C},2,2})\boldsymbol{\varepsilon}^n_u\right\|^2_{\ell^1(L^2)}$ $+\tau_p\tau_u\mu_u\left(\left\|\mu_p D^1_{\mathrm{B},2,1}\varepsilon^N_p\right\|^2 + \left\|\mu_p\left(3D^1_{\mathrm{B},2,1}\varepsilon^{N-1}_p - 4D^1_{\mathrm{B},2,1}\varepsilon^N_p\right)\right\|^2\right)$ $+\tau_p\tau_u\mu_p\left(\left\|\mu_u D^1_{\mathrm{B},2,1}\boldsymbol{\varepsilon}^N_u\right\|^2 + \left\|\mu_u\left(3D^1_{\mathrm{B},2,1}\boldsymbol{\varepsilon}^{N-1}_u - 4D^1_{\mathrm{B},2,1}\boldsymbol{\varepsilon}^N_u\right)\right\|^2\right)$ $+\tau_p\tau_u\mu_u\left(\left\|\nabla\cdot D^1_{\mathrm{B},1,1}\boldsymbol{\varepsilon}^1_u\right\|^2\delta t^2 + \left\|\nabla\cdot D^1_{\mathrm{F},2,1}\boldsymbol{\varepsilon}_u\right\|^2_{\ell^1(L^2)}\right)$ $+\tau_p\tau_u\mu_p\left(\left\|\nabla D^1_{\mathrm{B},1,1}\varepsilon^1_p\right\|^2\delta t^2 + \left\|\nabla D^1_{\mathrm{F},2,1}\varepsilon_p\right\|^2_{\ell^1(L^2)}\right)$ $+\frac{\delta t^4}{\mu_p}\left\|\mu_p\partial_{ttt}p^{\frac{1}{2}}\right\|^2\delta t^2 + \frac{\delta t^4}{\mu_p}\left\|\mu_p\partial_{ttt}p^n\right\|^2_{\ell^1(L^2)} + \frac{\delta t^4}{\mu_u}\left\|\mu_u\partial_{ttt}\boldsymbol{u}^{\frac{1}{2}}\right\|^2\delta t^2 + \frac{\delta t^4}{\mu_u}\left\|\mu_u\partial_{ttt}\boldsymbol{u}^n\right\|^2_{\ell^1(L^2)}$ $+\delta t^4\tau_p\left\|\mu_p\partial_{ttt}p^{\frac{1}{2}}\right\|^2\delta t + \delta t^4\tau_p\left\|\mu_p\partial_{ttt}p^n\right\|^2_{\ell^2(L^2)} + \delta t^4\tau_u\left\|\mu_u\partial_{ttt}\boldsymbol{u}^{\frac{1}{2}}\right\|^2\delta t + \delta t^4\tau_u\left\|\mu_u\partial_{ttt}\boldsymbol{u}^n\right\|^2_{\ell^2(L^2)}$ $+\delta t^4\tau_p\tau_u\mu_u\left(\left\|\mu_p\partial_{ttt}p^{\frac{1}{2}}\right\|^2 + \left\|\mu_p\partial_{tttt}p\right\|^2_{\ell^1(L^2)} + \left\|\mu_p\partial_{ttt}p\right\|^2_{L^\infty(L^2)}\right)$ $+\delta t^4\tau_p\tau_u\mu_p\left(\left\|\mu_u\partial_{ttt}\boldsymbol{u}^{\frac{1}{2}}\right\|^2 + \left\|\mu_u\partial_{tttt}\boldsymbol{u}\right\|^2_{\ell^1(L^2)} + \left\|\mu_u\partial_{ttt}\boldsymbol{u}\right\|^2_{L^\infty(L^2)}\right)$ |

Table 5
Error functions II: OSS formulation.

| Method | $E(h,\delta t)$ |
|---|---|
| BE | $E^2(h,\delta t) \coloneqq \mu_p \left\|\varepsilon_p\right\|^2_{\ell^\infty(L^2)} + \frac{1}{\tau_u}\left\|\boldsymbol{\varepsilon}_u\right\|^2_{\ell^2(\Upsilon,L^2(\Omega))} + \tau_p \left\|\mu_p D^1_{\mathrm{B},1,1}\varepsilon_p\right\|^2_{\ell^2(L^2)} + \tau_p \left\|\nabla\cdot\boldsymbol{\varepsilon}_u\right\|^2_{\ell^2(L^2)}$ $+\mu_u \left\|\boldsymbol{\varepsilon}_u\right\|^2_{\ell^\infty(L^2)} + \frac{1}{\tau_p}\left\|\varepsilon_p\right\|^2_{\ell^2(L^2)} + \tau_u \left\|\mu_u D^1_{\mathrm{B},1,1}\boldsymbol{\varepsilon}_u\right\|^2_{\ell^2(L^2)} + \tau_u \left\|\nabla\varepsilon_p\right\|^2_{\ell^2(L^2)}$ $+(1+\sigma)\kappa_p \left\|\varepsilon_p\right\|^2_{\ell^2(\Upsilon,L^2(\Gamma_\mathrm{o}))} + (1-\sigma)\kappa_u \left\|\boldsymbol{\varepsilon}_u\right\|^2_{\ell^2(\Upsilon,L^2(\Gamma_\mathrm{o}))}$ $+\frac{\delta t^2}{\mu_p}\left\|\mu_p\partial_{tt}p\right\|^2_{\ell^1(L^2)} + \frac{\delta t^2}{\mu_u}\left\|\mu_u\partial_{tt}\boldsymbol{u}\right\|^2_{\ell^1(L^2)} + \delta t^2\tau_p\left\|\mu_p\partial_{tt}p\right\|^2_{\ell^2(L^2)} + \delta t^2\tau_u\left\|\mu_u\partial_{tt}\boldsymbol{u}\right\|^2_{\ell^2(L^2)}$ |
| CN | $E^2(h,\delta t) \coloneqq \mu_p \left\|\varepsilon_p\right\|^2_{\ell^\infty(L^2)} + \mu_u \left\|\boldsymbol{\varepsilon}_u\right\|^2_{\ell^\infty(L^2)} + (1+\sigma)\kappa_p \left\|\varepsilon_p\right\|^2_{\ell^2(\Upsilon,L^2(\Gamma_\mathrm{o}))} + (1-\sigma)\kappa_u \left\|\boldsymbol{\varepsilon}_u\right\|^2_{\ell^2(\Upsilon,L^2(\Gamma_\mathrm{o}))}$ $+\frac{1}{\tau_u}\left\|\boldsymbol{\varepsilon}_u\right\|^2_{\ell^2(L^2)} + \tau_p \left\|\mu_p D^1_{\mathrm{B},1,1}\varepsilon_p\right\|^2_{\ell^2(L^2)} + \tau_p \left\|\nabla\cdot\boldsymbol{\varepsilon}_u\right\|^2_{\ell^2(L^2)}$ $+\frac{1}{\tau_p}\left\|\varepsilon_p\right\|^2_{\ell^2(L^2)} + \tau_u \left\|\mu_u D^1_{\mathrm{B},1,1}\boldsymbol{\varepsilon}_u\right\|^2_{\ell^2(L^2)} + \tau_u \left\|\nabla\varepsilon_p\right\|^2_{\ell^2(L^2)}$ $+\frac{\delta t^4}{\mu_p}\left\|\mu_p\partial_{ttt}p\right\|^2_{\ell^1(L^2)} + \delta t^4\tau_p\left\|\mu_p\partial_{ttt}p\right\|^2_{\ell^2(L^2)} + \frac{\delta t^4}{\mu_u}\left\|\mu_u\partial_{ttt}\boldsymbol{u}\right\|^2_{\ell^1(L^2)} + \delta t^4\tau_u\left\|\mu_u\partial_{ttt}\boldsymbol{u}\right\|^2_{\ell^2(L^2)}$ |
| BDF2 | $E^2(h,\delta t) \coloneqq \mu_p \left\|\varepsilon_p\right\|^2_{\ell^\infty(L^2)} + \mu_u \left\|\boldsymbol{\varepsilon}_u\right\|^2_{\ell^\infty(L^2)} + \frac{1}{\tau_u}\left\|\boldsymbol{\varepsilon}_u^{\frac{1}{2}}\right\|^2\delta t + \frac{1}{\tau_p}\left\|\varepsilon_p^{\frac{1}{2}}\right\|^2\delta t + \frac{1}{\tau_u}\left\|\boldsymbol{\varepsilon}_u\right\|^2_{\ell^2(L^2)} + \frac{1}{\tau_p}\left\|\varepsilon_p\right\|^2_{\ell^2(L^2)}$ $+(1+\sigma)\kappa_p \left\|\varepsilon_p\right\|^2_{\ell^2(\Upsilon,L^2(\Gamma_\mathrm{o}))} + (1-\sigma)\kappa_u \left\|\boldsymbol{\varepsilon}_u\right\|^2_{\ell^2(\Upsilon,L^2(\Gamma_\mathrm{o}))}$ $+\tau_p\left\|\mu_p D^1_{\mathrm{B},1,1}\varepsilon_p^1\right\|^2\delta t + \tau_p\left\|\nabla\cdot\boldsymbol{\varepsilon}_u^{\frac{1}{2}}\right\|^2\delta t + \tau_p\left\|\mu_p D^1_{\mathrm{B},2,1}\varepsilon_p^n\right\|^2_{\ell^2(L^2)} + \tau_p\left\|\nabla\cdot\boldsymbol{\varepsilon}_u\right\|^2_{\ell^2(L^2)}$ $+\tau_u\left\|\mu_u D^1_{\mathrm{B},1,1}\boldsymbol{\varepsilon}_u^1\right\|^2\delta t + \tau_u\left\|\nabla\varepsilon_p^{\frac{1}{2}}\right\|^2\delta t + \tau_u\left\|\mu_u D^1_{\mathrm{B},2,1}\boldsymbol{\varepsilon}_u^n\right\|^2_{\ell^2(L^2)} + \tau_u\left\|\nabla\varepsilon_p\right\|^2_{\ell^2(L^2)}$ $+\frac{\delta t^4}{\mu_p}\left\|\mu_p\partial_{ttt}p^{\frac{1}{2}}\right\|^2\delta t^2 + \frac{\delta t^4}{\mu_p}\left\|\mu_p\partial_{ttt}p^n\right\|^2_{\ell^1(L^2)} + \frac{\delta t^4}{\mu_u}\left\|\mu_p\partial_{ttt}\boldsymbol{u}^{\frac{1}{2}}\right\|^2\delta t^2 + \frac{\delta t^4}{\mu_u}\left\|\mu_u\partial_{ttt}\boldsymbol{u}^n\right\|^2_{\ell^1(L^2)}$ $+\delta t^4\left(\tau_p\left\|\mu_p\partial_{ttt}p^{\frac{1}{2}}\right\|^2\delta t + \tau_p\left\|\mu_p\partial_{ttt}p^n\right\|^2_{\ell^2(L^2)} + \tau_u\left\|\mu_u\partial_{ttt}\boldsymbol{u}^{\frac{1}{2}}\right\|^2\delta t + \tau_u\left\|\mu_u\partial_{ttt}\boldsymbol{u}^n\right\|^2_{\ell^2(L^2)}\right)$ |

where here and in what follows $\alpha_i > 0$ are reals appearing from Young's inequality. The 2nd and 4th terms are bounded in a similar manner and we just show how we bound the 2nd term:

$$
\begin{aligned}
&\sum_{n=1}^{N}\delta t\left({f_p}^n, \tau_p\nabla\cdot\tau_u\mu_u D^1_{\mathrm{B},1,1}\boldsymbol{u}_h^n\right)\\
&\quad= -\sum_{n=1}^{N}\delta t\left(D^1_{\mathrm{B},1,1}{f_p}^n, \tau_p\tau_u\mu_u\nabla\cdot\boldsymbol{u}_h^{n-1}\right) + \left({f_p}^N, \tau_p\tau_u\mu_u\nabla\cdot\boldsymbol{u}_h^N\right)\\
&\quad\lesssim \alpha_2\tau_p\tau_u\mu_u\left\|D^1_{\mathrm{B},1,1}f_p\right\|^2_{\ell^1(\Upsilon,L^2(\Omega))} + \alpha_3\tau_p\tau_u\mu_u\left\|f_p\right\|^2_{\ell^\infty(\Upsilon,L^2(\Omega))}\\
&\qquad+\frac{1}{\alpha_2}\tau_p\tau_u\mu_u\left\|\nabla\cdot\boldsymbol{u}_h\right\|^2_{\ell^\infty(\Upsilon,L^2(\Omega))} + \frac{1}{\alpha_3}\tau_p\tau_u\mu_u\left\|\nabla\cdot\boldsymbol{u}_h\right\|^2_{\ell^\infty(\Upsilon,L^2(\Omega))}.
\end{aligned}
\tag{41}
$$

Combining (38)–(41) and taking $\alpha_i$ large enough the proof is complete.

### 3.4.3. *Proof of convergence (32)*

Combining $\Lambda$-coercivity with $V = e$ and (34) we can arrive at

$$\left|\!\left|\!\left|e\right|\!\right|\!\right|^2 \lesssim \mathcal{B}_h(e,\Lambda(e)) = \mathcal{B}_h(\varepsilon,\Lambda(e)) + \mathcal{C}(U,\Lambda(e)).$$

The aim is to bound $e$ in terms of $\varepsilon$ and $U$. We first analyze the term containing $\mathcal{B}_h$ and then the term associated to the consistency error (33):

$$
\begin{aligned}
\mathcal{B}_h(\varepsilon, \Lambda(e)) &= \sum_{n=1}^{N} \delta t \left(\mu_p D^1_{\mathrm{B},1,1}\varepsilon_p^n + \nabla\cdot\boldsymbol{\varepsilon}_u^n, e_p^n + \tau_p\left(\mu_p D^1_{\mathrm{B},1,1} e_p^n + \nabla\cdot\boldsymbol{e}_u^n\right) + \tau_p\tau_u\mu_u\nabla\cdot D^1_{\mathrm{B},1,1}\boldsymbol{e}_u^n\right)\\
&\quad + \sum_{n=1}^{N} \delta t \left(\mu_u D^1_{\mathrm{B},1,1}\boldsymbol{e}_u^n + \nabla\varepsilon_p^n, \boldsymbol{e}_u^n + \tau_u\left(\mu_u D^1_{\mathrm{B},1,1}\boldsymbol{e}_u^n + \nabla e_p^n\right), +\tau_p\tau_u\mu_p\nabla D^1_{\mathrm{B},1,1} e_p^n\right)\\
&\le \sum_{n=1}^{N} \delta t \left[\frac{\alpha_1}{2\tau_p}\left\|\varepsilon_p^n\right\|^2 + \frac{\tau_p}{2\alpha_1}\left\|\mu_p D^1_{\mathrm{B},1,1} e_p^n + \nabla\cdot\boldsymbol{e}_u^n\right\|^2\right]\\
&\quad + \sum_{n=1}^{N} \delta t \left[\frac{\alpha_2}{2\tau_u}\left\|\boldsymbol{\varepsilon}_u^n\right\|^2 + \frac{\tau_u}{2\alpha_2}\left\|\mu_u D^1_{\mathrm{B},1,1}\boldsymbol{e}_u^n + \nabla e_p^n\right\|^2\right]\\
&\quad + \sum_{n=1}^{N} \delta t\tau_p \left[\frac{\alpha_3}{2}\left\|\mu_p D^1_{\mathrm{B},1,1}\varepsilon_p^n + \nabla\cdot\boldsymbol{\varepsilon}_u^n\right\|^2 + \frac{1}{2\alpha_3}\left\|\mu_p D^1_{\mathrm{B},1,1} e_p^n + \nabla\cdot\boldsymbol{e}_u^n\right\|^2\right]\\
&\quad + \sum_{n=1}^{N} \delta t\tau_u \left[\frac{\alpha_4}{2}\left\|\mu_u D^1_{\mathrm{B},1,1}\boldsymbol{e}_u^n + \nabla\varepsilon_p^n\right\|^2 + \frac{1}{2\alpha_4}\left\|\mu_u D^1_{\mathrm{B},1,1}\boldsymbol{e}_u^n + \nabla e_p^n\right\|^2\right]\\
&\quad + \sum_{n=1}^{N} \delta t \left(\mu_p D^1_{\mathrm{B},1,1}\varepsilon_p^n + \nabla\cdot\boldsymbol{\varepsilon}_u^n, \tau_p\tau_u\mu_u\nabla\cdot D^1_{\mathrm{B},1,1}\boldsymbol{e}_u^n\right)\\
&\quad + \sum_{n=1}^{N} \delta t \left(\mu_u D^1_{\mathrm{B},1,1}\boldsymbol{e}_u^n + \nabla\varepsilon_p^{n+1}, \tau_p\tau_u\mu_p\nabla D^1_{\mathrm{B},1,1} e_p^n\right).
\end{aligned}
$$

The only terms missing to bound are the last two ones. Both are bound similarly and we will only show how the first one is bounded. The first part is bounded as

$$
\begin{aligned}
&\sum_{n=1}^{N} \delta t \left(\mu_p D^1_{\mathrm{B},1,1}\varepsilon_p^n, \tau_p\tau_u\mu_u\nabla\cdot D^1_{\mathrm{B},1,1}\boldsymbol{e}_u^n\right)\\
&\quad = \tau_p\tau_u\mu_u\left[\left(\mu_p D^1_{\mathrm{B},1,1}\varepsilon_p^N, \nabla\cdot\boldsymbol{e}_u^N\right) - \left(\mu_p D^1_{\mathrm{B},1,1}\varepsilon_p^1, \nabla\cdot\boldsymbol{e}_u^0\right)\right] - \sum_{n=1}^{N-1}\delta t\tau_p\tau_u\mu_u\left(\mu_p D^2_{\mathrm{C},2,1}\varepsilon_p^n, \nabla\cdot\boldsymbol{e}_u^n\right)\\
&\quad \le \tau_p\tau_u\mu_u\left[\frac{\alpha_5}{2}\left\|\mu_p D^1_{\mathrm{B},1,1}\varepsilon_p^N\right\|^2 + \frac{1}{2\alpha_5}\left\|\nabla\cdot\boldsymbol{e}_u^N\right\|^2\right]\\
&\qquad + \tau_p\tau_u\mu_u\left[\frac{\alpha_6}{2}\left\|\mu_p D^2_{\mathrm{C},2,1}\varepsilon_p\right\|^2_{\ell^1(L^2)} + \frac{1}{2\alpha_6}\left\|\nabla\cdot\boldsymbol{e}_u\right\|^2_{\ell^\infty(L^2)}\right],
\end{aligned}
$$

and the second part is bounded as

$$
\begin{aligned}
&\sum_{n=1}^{N} \delta t \left(\nabla\cdot\boldsymbol{\varepsilon}_u^n, \tau_p\tau_u\mu_u\nabla\cdot D^1_{\mathrm{B},1,1}\boldsymbol{e}_u^n\right)\\
&\quad = \tau_p\tau_u\mu_u\left[\left(\nabla\cdot\boldsymbol{\varepsilon}_u^N, \nabla\cdot\boldsymbol{e}_u^N\right) - \left(\nabla\cdot\boldsymbol{\varepsilon}_u^0, \nabla\cdot\boldsymbol{e}_u^0\right)\right] - \sum_{n=1}^{N}\delta t\left(\nabla\cdot D^1_{\mathrm{B},1,1}\boldsymbol{\varepsilon}_u^n, \tau_p\tau_u\mu_u\nabla\cdot\boldsymbol{e}_u^n\right)\\
&\quad \le \tau_p\tau_u\mu_u\left[\frac{\alpha_7}{2}\left\|\nabla\cdot\boldsymbol{\varepsilon}_u^N\right\|^2 + \frac{1}{2\alpha_7}\left\|\nabla\cdot\boldsymbol{e}_u^N\right\|^2 + \frac{\alpha_8}{2}\left\|\nabla\cdot D^1_{\mathrm{B},1,1}\boldsymbol{\varepsilon}_u\right\|^2_{\ell^1(L^2)} + \frac{1}{2\alpha_8}\left\|\nabla\cdot\boldsymbol{e}_u\right\|^2_{\ell^\infty(L^2)}\right].
\end{aligned}
$$

This completes the bounding of $\mathcal{B}_h$. Now let us bound the consistency error (33):

$$\begin{aligned}
&\mathcal{C}(U, \Lambda(e)) = \mathcal{L}_h(\Lambda(e)) - \mathcal{B}_h(U, \Lambda(e)) \\
&\quad = -\sum_{n=1}^{N} \delta t \left(\mu_p D^1_{\mathrm{B},1,1} p^n + \nabla\cdot \boldsymbol{u}^n, e_p^n + \tau_p \left(\mu_p D^1_{\mathrm{B},1,1} e_p^n + \nabla\cdot \boldsymbol{e}_u^n\right) + \tau_p\tau_u\mu_u \nabla\cdot D^1_{\mathrm{B},1,1}\boldsymbol{e}_u^n\right) \\
&\qquad - \sum_{n=1}^{N} \delta t \left(\mu_u D^1_{\mathrm{B},1,1}\boldsymbol{u}^n + \nabla p^n, \boldsymbol{e}_u^n + \tau_u \left(\mu_u D^1_{\mathrm{B},1,1}\boldsymbol{e}_u^n + \nabla e_p^n\right) + \tau_p\tau_u\mu_p \nabla D^1_{\mathrm{B},1,1} e_p^n\right).
\end{aligned}$$

Both terms are bounded similarly and we only show how the first one is bounded. Let us start with its first part

$$\begin{aligned}
-\sum_{n=1}^{N} \delta t \left(\mu_p D^1_{\mathrm{B},1,1} p^n + \nabla\cdot \boldsymbol{u}^n, e_p^n\right) &\le \frac{\alpha_9}{2}\frac{\delta t^2}{\mu_p}\left[\sum_{n=1}^{N}\left\|\mu_p D^1_{\mathrm{B},1,1} p^n + \nabla\cdot\boldsymbol{u}^n\right\|\right]^2 + \frac{1}{2\alpha_9}\mu_p \left\|e_p\right\|^2_{\ell^\infty(L^2)} \\
&\le \frac{\alpha_9}{2}\frac{\delta t^2}{\mu_p}\left[\sum_{n=1}^{N}\left\|\mu_p D^1_{\mathrm{B},1,1} p^n - \mu_p\partial_t p^n\right\|\right]^2 + \frac{1}{2\alpha_9}\mu_p \left\|e_p\right\|^2_{\ell^\infty(L^2)} \\
&\le \frac{\alpha_9}{2}\frac{\delta t^2}{\mu_p}\left\|\mu_p\partial_{tt} p^n\right\|^2_{\ell^1(L^2)} + \frac{1}{2\alpha_9}\mu_p \left\|e_p\right\|^2_{\ell^\infty(L^2)}.
\end{aligned}$$

The second part can be bounded as

$$\begin{aligned}
&-\sum_{n=1}^{N} \delta t \left(\mu_p D^1_{\mathrm{B},1,1} p^n + \nabla\cdot \boldsymbol{u}^n, \tau_p\left(\mu_p D^1_{\mathrm{B},1,1} e_p^n + \nabla\cdot\boldsymbol{e}_u^n\right)\right) \\
&\le \frac{\alpha_{10}}{2}\sum_{n=1}^{N}\delta t\tau_p\left\|\mu_p D^1_{\mathrm{B},1,1} p^n - \mu_p\partial_t p^n\right\|^2 + \frac{1}{2\alpha_{10}}\sum_{n=1}^{N}\delta t\tau_p\left\|\mu_p D^1_{\mathrm{B},1,1} e_p^n + \nabla\cdot\boldsymbol{e}_u^n\right\|^2 \\
&\le \frac{\alpha_{10}}{2}\delta t^2\tau_p\left\|\mu_p\partial_{tt} p^n\right\|^2_{\ell^2(\Upsilon,L^2(\Omega))} + \frac{1}{2\alpha_{10}}\tau_p\left\|\mu_p D^1_{\mathrm{B},1,1} e_p^n + \nabla\cdot\boldsymbol{e}_u^n\right\|^2_{\ell^2(\Upsilon,L^2(\Omega))}.
\end{aligned}$$

The third part can be bounded as

$$\begin{aligned}
&-\sum_{n=1}^{N} \delta t \left(\mu_p D^1_{\mathrm{B},1,1} p^n + \nabla\cdot \boldsymbol{u}^n, \tau_p\tau_u\mu_u\nabla\cdot D^1_{\mathrm{B},1,1}\boldsymbol{e}_u^n\right) \\
&\quad = \tau_p\tau_u\mu_u\left[\left(\mu_p D^1_{\mathrm{B},1,1} p^N + \nabla\cdot\boldsymbol{u}^N, \nabla\cdot\boldsymbol{e}_u^N\right) - \left(\mu_p D^1_{\mathrm{B},1,1} p^1 + \nabla\cdot\boldsymbol{u}^0, \nabla\cdot\boldsymbol{e}_u^0\right)\right] \\
&\qquad - \tau_p\tau_u\mu_u\left[\sum_{n=1}^{N-1}\delta t\left(\mu_p D^2_{\mathrm{C},2,1} p^n + \nabla\cdot D^1_{\mathrm{B},1,1}\boldsymbol{u}^n, \nabla\cdot\boldsymbol{e}_u^n\right) + \delta t\left(\nabla\cdot D^1_{\mathrm{B},1,1}\boldsymbol{u}^1, \nabla\cdot\boldsymbol{e}_u^0\right)\right] \\
&\quad \le \tau_p\tau_u\mu_u\left[\frac{\alpha_{11}}{2}\left\|\mu_p D^1_{\mathrm{B},1,1} p^N + \nabla\cdot\boldsymbol{u}^N\right\|^2 + \frac{1}{2\alpha_{11}}\left\|\nabla\cdot\boldsymbol{e}_u^N\right\|^2\right] \\
&\qquad + \tau_p\tau_u\mu_u\frac{\alpha_{12}}{2}\left[\sum_{n=1}^{N-1}\delta t\left\|\mu_p D^2_{\mathrm{C},2,1} p^n + \nabla\cdot D^1_{\mathrm{B},1,1}\boldsymbol{u}^n\right\|\right]^2 + \tau_p\tau_u\mu_u\frac{1}{2\alpha_{12}}\left\|\nabla\cdot\boldsymbol{e}_u\right\|^2 \\
&\quad \le \tau_p\tau_u\mu_u\left[\frac{\alpha_{11}}{2}\delta t^2\left\|\mu_p\partial_{tt} p^N\right\|^2 + \frac{1}{2\alpha_{11}}\left\|\nabla\cdot\boldsymbol{e}_u^N\right\|^2\right] \\
&\qquad + \tau_p\tau_u\mu_u\left[\frac{\alpha_{12}}{2}\delta t^2\left\|\mu_p\partial_{ttt} p\right\|^2_{\ell^1(\Upsilon,L^2(\Omega))} + \frac{1}{2\alpha_{12}}\left\|\nabla\cdot\boldsymbol{e}_u\right\|^2_{\ell^\infty(\Upsilon,L^2(\Omega))}\right].
\end{aligned}$$

Combining all bounds the proof is complete.

Table 6
Convergence rates for ASGS-BE and OSS-BE according to variational form.

| Variational form | I | II | III |
|---|---|---|---|
| $\left\|\xi_p^n\right\|_{\ell^\infty(L^2)}$, $\left\|\xi_u^n\right\|_{\ell^\infty(L^2)}$ | $h^{k+\frac{1}{2}} + h^{l+\frac{1}{2}} + \delta t + h^{\frac{1}{2}}\delta t$ | $h^{k+\frac{1}{2}} + h^{l} + \delta t$ | $h^{k} + h^{l+\frac{1}{2}} + \delta t$ |
| $\left\|\mu_u D^1_{\mathrm{B},1,1}\xi_u^n + \nabla\xi_p^n\right\|_{\ell^2(L^2)}$ | $h^{k} + h^{l} + h^{-\frac{1}{2}}\delta t + \delta t$ | $h^{k-\frac{1}{2}} + h^{l-1} + h^{-1}\delta t$ | $h^{k} + h^{l+\frac{1}{2}} + \delta t$ |
| $\left\|\mu_p D^1_{\mathrm{B},1,1}\xi_p^n + \nabla\cdot\xi_u^n\right\|_{\ell^2(L^2)}$ | $h^{k} + h^{l} + h^{-\frac{1}{2}}\delta t + \delta t$ | $h^{k+\frac{1}{2}} + h^{l} + \delta t$ | $h^{k-1} + h^{l-\frac{1}{2}} + h^{-1}\delta t$ |
| Best $k$, $l$, $h$-$\delta t$ | $k = l$, $\delta t \sim h^{k+\frac{1}{2}}$ | $k+\frac{1}{2} = l$, $\delta t \sim h^{l}$<br>$k = l$, $\delta t \sim h^{l}$<br>$k+1 = l$, $\delta t \sim h^{l-\frac{1}{2}}$ | $k = l+\frac{1}{2}$, $\delta t \sim h^{k}$<br>$k = l$, $\delta t \sim h^{k}$<br>$k = l+1$, $\delta t \sim h^{k-\frac{1}{2}}$ |

Table 7
Convergence rates for ASGS-CN and OSS-CN according to variational form.

| Variational form | I | II | III |
|---|---|---|---|
| $\left\|\xi_p^n\right\|_{\ell^\infty(L^2)}$, $\left\|\xi_u^n\right\|_{\ell^\infty(L^2)}$ | $h^{k+\frac{1}{2}} + h^{l+\frac{1}{2}} + \delta t^2 + h^{\frac{1}{2}}\delta t^2$ | $h^{k+\frac{1}{2}} + h^{l} + \delta t^2$ | $h^{k} + h^{l+\frac{1}{2}} + \delta t^2$ |
| $\left\|\mu_u D^1_{\mathrm{B},1,1}\xi_u^n + \nabla\xi_p^{n-\frac{1}{2}}\right\|_{\ell^2(L^2)}$ | $h^{k} + h^{l} + h^{-\frac{1}{2}}\delta t^2 + \delta t^2$ | $h^{k-\frac{1}{2}} + h^{l-1} + h^{-1}\delta t^2$ | $h^{k} + h^{l+\frac{1}{2}} + \delta t^2$ |
| $\left\|\mu_p D^1_{\mathrm{B},1,1}\xi_p^n + \nabla\cdot\xi_u^{n-\frac{1}{2}}\right\|_{\ell^2(L^2)}$ | $h^{k} + h^{l} + h^{-\frac{1}{2}}\delta t^2 + \delta t^2$ | $h^{k+\frac{1}{2}} + h^{l} + \delta t^2$ | $h^{k-1} + h^{l-\frac{1}{2}} + h^{-1}\delta t^2$ |
| Best $k$, $l$, $h$-$\delta t$ | $k = l$, $\delta t^2 \sim h^{k+\frac{1}{2}}$ | $k+\frac{1}{2} = l$, $\delta t^2 \sim h^{l}$<br>$k = l$, $\delta t^2 \sim h^{l}$<br>$k+1 = l$, $\delta t^2 \sim h^{l-\frac{1}{2}}$ | $k = l+\frac{1}{2}$, $\delta t^2 \sim h^{k}$<br>$k = l$, $\delta t^2 \sim h^{k}$<br>$k = l+1$, $\delta t^2 \sim h^{k-\frac{1}{2}}$ |

### 3.5. Accuracy of the fully discrete methods

Let $k$ be the order of $p$-interpolation and $l$ the order of $\boldsymbol{u}$-interpolation. Analyzing the a priori error estimates (32) for the fully discrete methods with the error functions given in Tables 4 and 5 and assuming regular enough solutions, we can summarize the convergence rates as shown in Tables 6–8. We stress the fact that the convergence rates do depend on the choice of the stabilization parameters, and different convergence orders are obtained for the three discrete variational formulations above. Let us note that the time discretization schemes do not spoil the spatial convergence rates obtained in [10,11] for the time-continuous case. Let us mention that the negative powers of $h$ appear due to some terms in the error function having $\tau_p$ or $\tau_u$ dividing (see Tables 4 and 5). Obviously, an appropriate $(\delta t, h)$ relationship should be chosen to have convergence.

## 4. Fourier analysis

We show now the results of a Fourier analysis (or von Neumann analysis) in 1D using linear (P1) elements, which serve to study dispersion, dissipation, and stability of the numerical schemes. The analysis is done in an unbounded domain with no forcing terms, but with non-zero initial conditions. The mesh is taken uniform, of size $h$, and the time step is $\delta t$. We focus on variational form I because it has the best convergence properties, as shown in the previous analysis.

Let us consider a solution of the form $p = C_p \mathrm{e}^{\mathrm{i}(kx-\omega t)}$ and $u = C_p \mu_p^{1/2} \mu_u^{-1/2} \mathrm{e}^{\mathrm{i}(kx-\omega t)}$, where $C_p$ is an arbitrary constant such that $[p] = [C_p]$, $[\cdot]$ standing for dimensional group, $\omega$ is the angular frequency (temporal frequency) and $k$ is the (angular) wavenumber (spatial frequency). It can be checked that this plane wave is solution of the wave equation in mixed form. The angular frequency and wavenumber are related through the wave speed as $\omega = kc$.

We denote by $\Re(\cdot)$ and $\Im(\cdot)$ the real and imaginary parts of a complex number respectively. The stability conditions can be summarized as follows: $\Im(kh) \geq 0$ or $\Im(\omega\delta t) \leq 0$, where $k$ and $\omega$ are the semi-discrete or fully-discrete wavenumber and angular frequency respectively.

Table 8
Convergence rates for ASGS-BDF2 and OSS-BDF2 according to variational form.

| Variational form | I | II | III |
|---|---|---|---|
| $\left\|\xi_p^n\right\|_{\ell^\infty(L^2)}$, $\left\|\xi_u^n\right\|_{\ell^\infty(L^2)}$ | $h^{k+\frac{1}{2}}+h^{l+\frac{1}{2}}+\delta t^2$ | $h^{k+\frac{1}{2}}+h^{l}+\delta t^2$ | $h^{k}+h^{l+\frac{1}{2}}+\delta t^2$ |
| $\left\|\mu_u D^1_{\mathrm{B},2,1}\xi_u^n+\nabla\xi_p^n\right\|_{\ell^2(L^2)}$ | $h^{k}+h^{l}+h^{-\frac{1}{2}}\delta t^2$ | $h^{k-\frac{1}{2}}+h^{l-1}+h^{-1}\delta t^2$ | $h^{k}+h^{l+\frac{1}{2}}+\delta t^2$ |
| $\left\|\mu_p D^1_{\mathrm{B},2,1}\xi_p^n+\nabla\cdot\xi_u^n\right\|_{\ell^2(L^2)}$ | $h^{k}+h^{l}+h^{-\frac{1}{2}}\delta t^2$ | $h^{k+\frac{1}{2}}+h^{l}+\delta t^2$ | $h^{k-1}+h^{l-\frac{1}{2}}+h^{-1}\delta t^2$ |
| Best $k$, $l$, $h$-$\delta t$ | $k=l$, $\delta t^2\sim h^{k+\frac{1}{2}}$ | $k+\frac{1}{2}=l$, $\delta t^2\sim h^{l}$<br>$k=l$, $\delta t^2\sim h^{l}$<br>$k+1=l$, $\delta t^2\sim h^{l-\frac{1}{2}}$ | $k=l+\frac{1}{2}$, $\delta t^2\sim h^{k}$<br>$k=l$, $\delta t^2\sim h^{k}$<br>$k=l+1$, $\delta t^2\sim h^{k-\frac{1}{2}}$ |

For 1D P1 elements of size diam $K=h$ we will need the following element matrices:

$$\int_K N_i N_j\Big|_{i,j=1,2}=\frac{h}{6}\begin{pmatrix}2&1\\1&2\end{pmatrix},\qquad \int_K N_i\partial_x N_j\Big|_{i,j=1,2}=\frac{1}{2}\begin{pmatrix}-1&1\\-1&1\end{pmatrix},$$
$$\int_K \partial_x N_i N_j\Big|_{i,j=1,2}=\frac{1}{2}\begin{pmatrix}-1&-1\\1&1\end{pmatrix},\qquad \int_K \partial_x N_i\partial_x N_j\Big|_{i,j=1,2}=\frac{1}{h}\begin{pmatrix}1&-1\\-1&1\end{pmatrix},$$

where $N_i$ is the shape function of node $i$ (in element $K$). When assembled for just two elements sharing a generic node they give, respectively,

$$M_p=M_u=\frac{h}{6}\begin{pmatrix}2&1&0\\1&4&1\\0&2&1\end{pmatrix},\qquad K_p=K_u=\frac{1}{2}\begin{pmatrix}-1&1&0\\-1&0&1\\0&-1&1\end{pmatrix},$$
$$M_{S,p}=M_{S,u}=\frac{1}{2}\begin{pmatrix}-1&-1&0\\1&0&-1\\0&1&1\end{pmatrix},\qquad K_{S,p}=K_{S,u}=\frac{1}{h}\begin{pmatrix}1&-1&0\\-1&2&-1\\0&-1&1\end{pmatrix}.$$

Additionally, we define the lumped mass matrices

$$\widetilde{M}_p=\widetilde{M}_u=\frac{h}{2}\begin{pmatrix}1&0&0\\0&2&0\\0&0&1\end{pmatrix}.$$

First we will analyze the time semi-discretization, then the space semi-discretization and finally the full discretization. The time discretizations to be considered are the $\theta$ and BDF2 methods, whereas the space discretizations to be analyzed are stabilized FE methods (ASGS and OSS). We will often take $t_n=n\delta t$ and $x_j=jh$, where $n$ is the time step and $j$ is the mesh point.

### 4.1. Time semi-discretization

Let us start considering the effect of the time discretization only, without discretizing in space. Let us take $\omega_{\delta t}=k_{\delta t}c_{\delta t}$ and $k_{\delta t}=k$, where the subscript $\delta t$ denotes temporal semi-discretization. We take a solution (mode) of the form

$$\left[P^n(x),U^n(x)\right]=\phi_k \mathrm{e}^{\mathrm{i}(kx-\omega_{\delta t}t_n)}\left[1,\mu_p^{1/2}\mu_u^{-1/2}\right],\tag{42}$$

where $\phi_k$ is a constant that describes the amplitude at $t_n=0$.

The semi-discrete problem using the $\theta$ method is as follows:

$$\frac{\mu_p}{\delta t}(P^{n+1}-P^n)+\theta\frac{\mathrm{d}}{\mathrm{d}x}U^{n+1}+(1-\theta)\frac{\mathrm{d}}{\mathrm{d}x}U^n=0,$$
$$\frac{\mu_u}{\delta t}(U^{n+1}-U^n)+\theta\frac{\mathrm{d}}{\mathrm{d}x}P^{n+1}+(1-\theta)\frac{\mathrm{d}}{\mathrm{d}x}P^n=0,$$

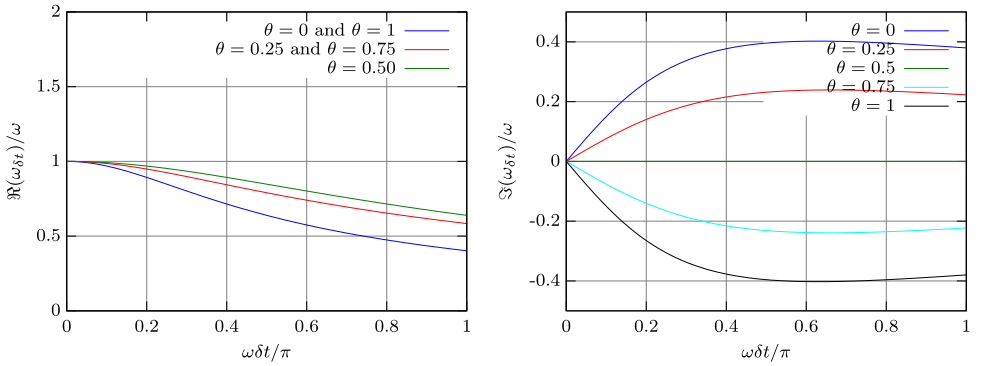


Fig. 1. $\theta$-method time semi-discretization.

where $0 \leq \theta \leq 1$ is a parameter. The backward Euler method corresponds to $\theta = 1$, the forward Euler method to $\theta = 0$ and the trapezoidal rule to $\theta = 0.5$. Replacing $[P^n, U^n]$ from (42) we have:

$$\frac{\mu_p}{\delta t}\left(\mathrm{e}^{-\mathrm{i}\omega_{\delta t}\delta t} - 1\right) + \mu_p^{1/2}\mu_u^{-1/2}\left(\mathrm{i}k\theta\mathrm{e}^{-\mathrm{i}\omega_{\delta t}\delta t} + \mathrm{i}k(1-\theta)\right) = 0,$$
$$\frac{\mu_u}{\delta t}\mu_p^{1/2}\mu_u^{-1/2}\left(\mathrm{e}^{-\mathrm{i}\omega_{\delta t}\delta t} - 1\right) + \mathrm{i}k\theta\mathrm{e}^{-\mathrm{i}\omega_{\delta t}\delta t} + \mathrm{i}k(1-\theta) = 0.$$

Both equations are equivalent, so we just analyze one of them. We have that

$$\omega_{\delta t}\delta t = \frac{-1}{\mathrm{i}}\log\left(\frac{1-(1-\theta)\mathrm{i}\omega\delta t}{1+\mathrm{i}\omega\delta t\theta}\right).$$

The numerical angular frequency, $\omega_{\delta t}$, is not always real, it is complex for $\theta \neq 0.5$. It can be shown that the angular frequency error is 2nd order in $\omega\delta t$ for $\theta = 0.5$ and only 1st order in $\omega\delta t$ for $\theta \neq 0.5$. Fig. 1 shows the angular frequency ratio $\omega_{\delta t}/\omega$ for $0 \leq \omega\delta t/\pi \leq 1$. It can be seen that the $\theta$-method is unconditionally stable for $\theta \geq 0.5$.

On the other hand, the semi-discrete problem using BDF2 is:

$$\frac{\mu_p}{2\delta t}(3P^{n+1} - 4P^n + P^{n-1}) + \frac{\mathrm{d}}{\mathrm{d}x}U^{n+1} = 0,$$
$$\frac{\mu_u}{2\delta t}(3U^{n+1} - 4U^n + U^{n-1}) + \frac{\mathrm{d}}{\mathrm{d}x}P^{n+1} = 0.$$

Following a similar procedure as for the $\theta$ method we arrive at

$$\omega_{\delta t}\delta t = \frac{1}{\mathrm{i}}\log(2 \pm \sqrt{1-2\mathrm{i}\omega\delta t}).$$

The numerical angular frequency is complex. The root corresponding to $+\sqrt{}$ is spurious, hence we just plot the root corresponding to $-\sqrt{}$. It can be shown that the angular frequency error is 2nd order in $\omega\delta t$. Fig. 2 shows the angular frequency ratio $\omega_{\delta t}/\omega$ for $0 \leq \omega\delta t/\pi \leq 1$. It can be seen that the BDF2 method is unconditionally stable.

Now, let us compare the $\theta$-method with $\theta = 1/2$ and BDF2. Fig. 3 compares both methods. It can be seen that the $\theta$-method with $\theta = 1/2$ outperforms BDF2 for the wave equation in mixed form both in terms of dispersion and dissipation.

### 4.2. Space semi-discretization

We analyze now the wave equation in mixed form when the spatial discretization is done using the ASGS and the OSS method. We take $\omega_h = k_h c_h$ and $\omega_h = \omega$, where the subscript $h$ denotes spatial semi-discretization. We take now

$$\left[P_j(t), U_j(t)\right] = \phi_\omega \mathrm{e}^{\mathrm{i}(k_h x_j - \omega t)}\left[1, \mu_p^{1/2}\mu_u^{-1/2}\right], \tag{43}$$

where $\phi_\omega$ is a constant that describes the amplitude at $t = 0$.

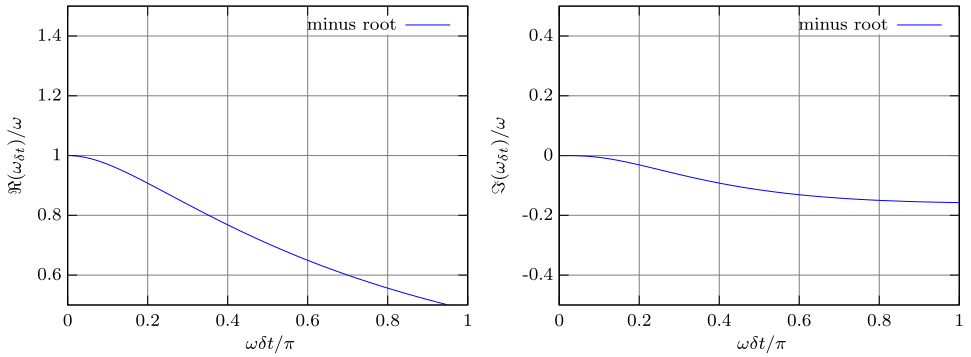


Fig. 2. BDF2 time semi-discretization.

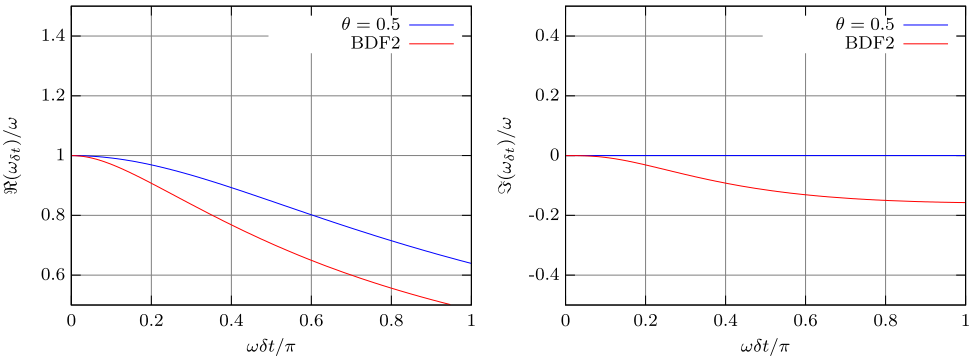


Fig. 3. Time semi-discretization comparison.

For the ASGS method, the semi-discrete problem has the matrix structure:

$$\mu_p M_p \frac{\mathrm{d}P}{\mathrm{d}t} + K_u U + \tau_u \mu_u M_{S,u} \frac{\mathrm{d}U}{\mathrm{d}t} + \tau_u K_{S,p} P = 0,$$
$$\mu_u M_u \frac{\mathrm{d}U}{\mathrm{d}t} + K_p P + \tau_p \mu_p M_{S,p} \frac{\mathrm{d}P}{\mathrm{d}t} + \tau_p K_{S,u} U = 0,$$

where a subscript $S$ has been introduced in the matrices with contributions from the stabilization terms. In these equations, $P$ and $U$ do not denote the sequence of solutions in time, but the array of nodal unknowns with time-continuous components. The meaning of $P$ and $U$ in what follows will be determined by the context. We just analyze one of the previous equations because they are equivalent. The $j$th row of the first system of equations is

$$\mu_p \frac{h}{6}\left(\frac{\mathrm{d}}{\mathrm{d}t}P_{j-1} + 4\frac{\mathrm{d}}{\mathrm{d}t}P_j + \frac{\mathrm{d}}{\mathrm{d}t}P_{j+1}\right) + \frac{1}{2}(-U_{j-1} + U_{j+1})$$
$$+ \tau_u \mu_u \frac{1}{2}\left(\frac{\mathrm{d}}{\mathrm{d}t}U_{j-1} - \frac{\mathrm{d}}{\mathrm{d}t}U_{j+1}\right) + \tau_u \frac{1}{h}\left(-P_{j-1} + 2P_j - P_{j+1}\right) = 0.$$

Replacing $[P_j, U_j]$ from (43) we have:

$$-\mathrm{i}\omega\mu_p \frac{h}{6}\left(\mathrm{e}^{-\mathrm{i}k_h h} + 4 + \mathrm{e}^{\mathrm{i}k_h h}\right) + \frac{1}{2}\mu_p^{1/2}\mu_u^{-1/2}\left(-\mathrm{e}^{-\mathrm{i}k_h h} + \mathrm{e}^{\mathrm{i}k_h h}\right)$$
$$-\frac{1}{2}\mathrm{i}\omega\tau_u\mu_p^{1/2}\mu_u^{1/2}\left(\mathrm{e}^{-\mathrm{i}k_h h} - \mathrm{e}^{\mathrm{i}k_h h}\right) + \frac{1}{h}\tau_u\left(-\mathrm{e}^{-\mathrm{i}k_h h} + 2 - \mathrm{e}^{\mathrm{i}k_h h}\right) = 0,$$
$$\frac{k_h}{k} = -\frac{\mathrm{i}}{kh}\log\left(\frac{-(4kh + 12\mathrm{i}C_\tau) \pm \sqrt{36(kh)^2C_\tau^2 + 72\mathrm{i}khC_\tau + 12(kh)^2 - 36}}{2(kh + 3\mathrm{i} - 3khC_\tau - 6\mathrm{i}C_\tau)}\right).$$

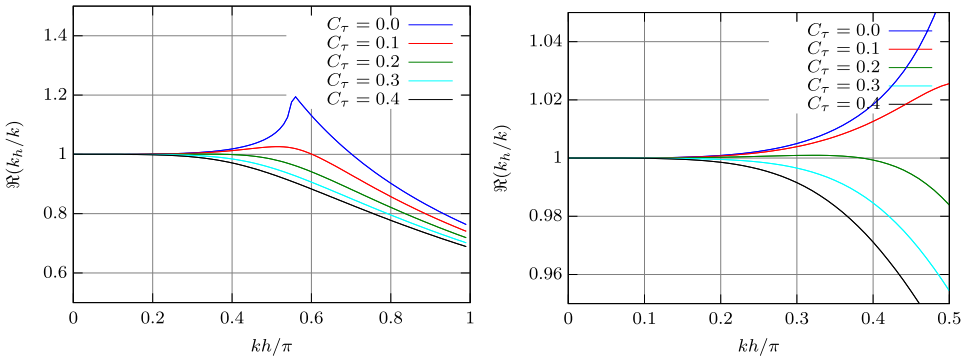


Fig. 4. ASGS space semi-discretization: real part of the wavenumber ratio (the right picture is a zoom of the left).

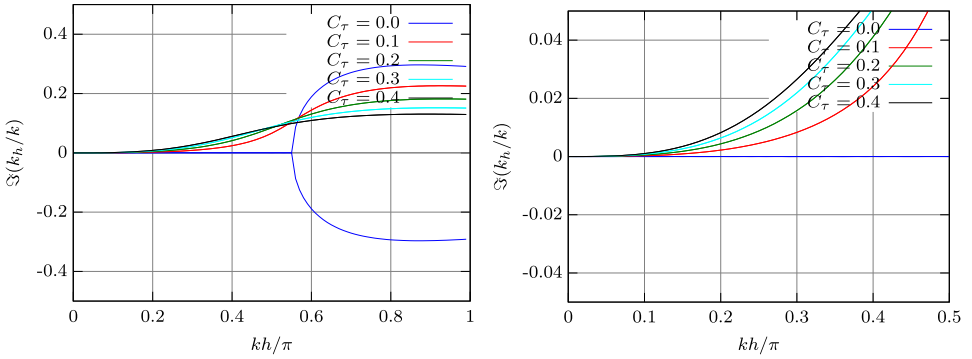


Fig. 5. ASGS space semi-discretization: imaginary part of the wavenumber ratio (the right picture is a zoom of the left).

The Maclaurin series for the real and imaginary parts are:

$$\frac{\Re(k_h)}{k} = 1 - \frac{15C_\tau^2 - 1}{180}(kh)^4 + \frac{126C_\tau^4 - 63C_\tau^2 + 1}{1512}(kh)^6 + \cdots,$$
$$\frac{\Im(k_h)}{k} = \frac{C_\tau}{12}(kh)^3 - \frac{6C_\tau^3 - C_\tau}{72}(kh)^5 + \cdots.$$

It can be shown that $k_h$ is complex and that $\Re(k_h)$ is of order $(kh)^4$ for any $C_\tau$ and of order $(kh)^6$ for $C_\tau = 1/\sqrt{15} \approx 0.2582$. Additionally, $\Im(k_h)$ is of order $(kh)^3$ for any $C_\tau > 0$. Figs. 4 and 5 show the real and imaginary parts of the wavenumber ratio as a function of $kh/\pi$. It can be seen that the Galerkin method ($C_\tau = 0$) is unstable whereas the ASGS method is always stable.

Next, we analyze an OSS method in which a lumped mass matrix (diagonal) is used to project the residual. Additionally, as the projection with a lumped mass matrix is not exactly an $L^2$ projection, we keep the time derivatives in the residual. Non-lumped (consistent) mass matrices are used for time derivatives. Better than lumped mass matrix approximations to the $L^2$ projection can be used, but the results obtained are very similar. For instance we could use the family of banded approximate mass matrices from [31].

The matrix form of the semi-discrete problem is:

$$\mu_p M_p \frac{\mathrm{d}P}{\mathrm{d}t} + K_u U + \tau_u \mu_u M_{S,u} \frac{\mathrm{d}U}{\mathrm{d}t} + \tau_u K_{S,p} P - \tau_u M_{S,u} R_u = 0,$$
$$M_u R_u = \mu_u M_u \frac{\mathrm{d}}{\mathrm{d}t} U + K_p P,$$
$$\mu_u M_u \frac{\mathrm{d}U}{\mathrm{d}t} + K_p P + \tau_p \mu_p M_{S,p} \frac{\mathrm{d}P}{\mathrm{d}t} + \tau_p K_{S,u} U - \tau_p M_{S,p} R_p = 0,$$
$$M_p R_p = \mu_p M_p \frac{\mathrm{d}}{\mathrm{d}t} P + K_u U.$$

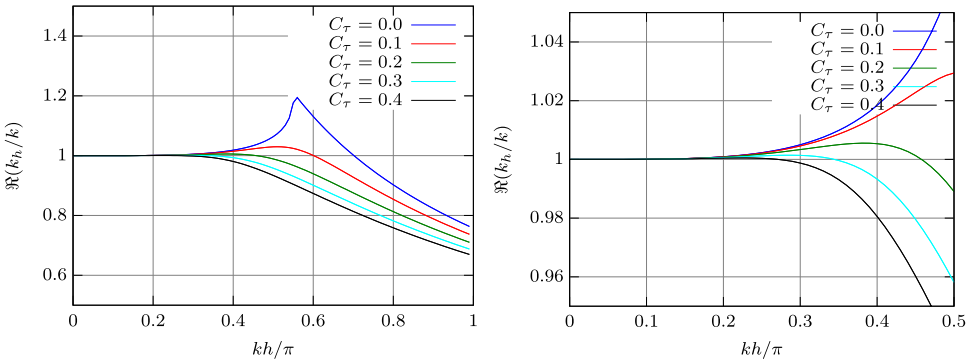


Fig. 6. OSS space semi-discretization: real part of the wavenumber ratio (the right picture is a zoom of the left).

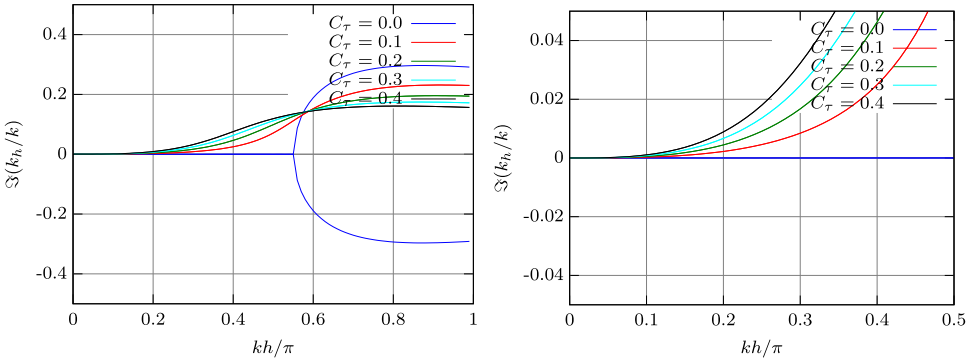


Fig. 7. OSS space semi-discretization: imaginary part of the wavenumber ratio (the right picture is a zoom of the left).

As we use a lumped projection, the semi-discrete problem reduces to:

$$\mu_p M_p \frac{\mathrm{d}P}{\mathrm{d}t} + K_u U + \tau_u \mu_u M_{S,u} \frac{\mathrm{d}U}{\mathrm{d}t} + \tau_u K_{S,p} P - \tau_u M_{S,u} \widetilde{M}_u^{-1} \left( \mu_u M_u \frac{\mathrm{d}}{\mathrm{d}t} U + K_p P \right) = 0,$$
$$\mu_u M_u \frac{\mathrm{d}U}{\mathrm{d}t} + K_p P + \tau_p \mu_p M_{S,p} \frac{\mathrm{d}P}{\mathrm{d}t} + \tau_p K_{S,u} U - \tau_p M_{S,p} \widetilde{M}_p^{-1} \left( \mu_p M_p \frac{\mathrm{d}}{\mathrm{d}t} P + K_u U \right) = 0.$$

Following similar steps as for the ASGS method, we arrive at the expression which relates $k_h h$ with $kh$:

$$2kh \left( \mathrm{e}^{\mathrm{i}k_h h} + 4\mathrm{e}^{2\mathrm{i}k_h h} + \mathrm{e}^{3\mathrm{i}k_h h} \right) + 6\mathrm{i} \left( -\mathrm{e}^{\mathrm{i}k_h h} + \mathrm{e}^{3\mathrm{i}k_h h} \right)$$
$$+ khC_\tau \left( -1 + 2\mathrm{e}^{\mathrm{i}k_h h} - 2\mathrm{e}^{3\mathrm{i}k_h h} + \mathrm{e}^{4\mathrm{i}k_h h} \right) + 3\mathrm{i}C_\tau \left( 1 - 4\mathrm{e}^{\mathrm{i}k_h h} + 6\mathrm{e}^{2\mathrm{i}k_h h} - 4\mathrm{e}^{3\mathrm{i}k_h h} + \mathrm{e}^{4\mathrm{i}k_h h} \right) = 0.$$

Figs. 6 and 7 show the real and imaginary parts of the wavenumber ratio as a function of $kh/\pi$. As before, the Galerkin method ($C_\tau = 0$) is unstable whereas the OSS method is always stable.

### 4.3. Space–time discretization

Finally, we analyze the fully discrete problems arising from the combination of time discretizations ($\theta$ and BDF2) and space discretizations (ASGS and OSS). Thus, in total we will analyze four fully discrete problems. We take $\omega_* = k_* c_*$ and $k_* = k$. The subscript $*$ denotes full discretization. We take a mode of the form

$$\left[ P_j^n, U_j^n \right] = \phi_k \mathrm{e}^{\mathrm{i}(kx_j - \omega_* t_n)} \left[ 1, \mu_p^{1/2} \mu_u^{-1/2} \right], \tag{44}$$

where $\phi_k$ describes the amplitude at $t_n = 0$.

Let us define $r$ as the Courant or CFL number as

$$r := c\delta t / h. \tag{45}$$

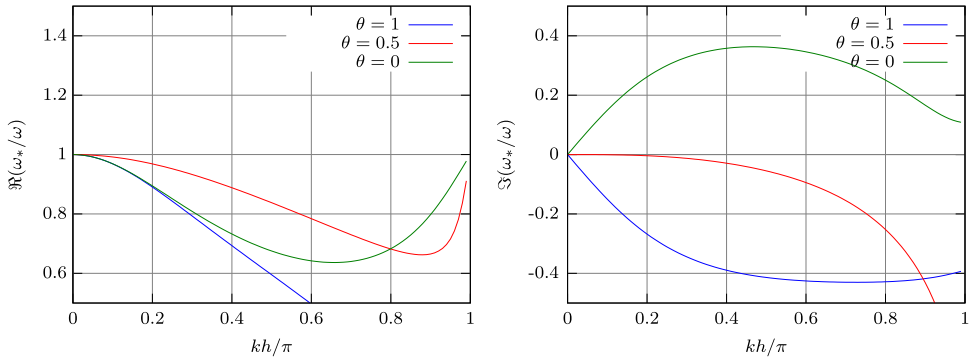


Fig. 8. ASGS + $\theta$ for $r = 1$ and $C_\tau = 0.2$.

First, we consider the ASGS formulation for the space discretization. With regard to the time integration, we first consider the $\theta$-method. The fully discrete problem is:

$$\begin{aligned}
&\frac{\mu_p}{\delta t} M_p \left(P^{n+1} - P^n\right) + \tau_u \frac{\mu_u}{\delta t} M_{S,u} \left(U^{n+1} - U^n\right) + \theta \left(K_u U^{n+1} + \tau_u K_{S,p} P^{n+1}\right) \\
&\quad + (1-\theta)\left(K_u U^n + \tau_u K_{S,p} P^n\right) = 0, \\
&\frac{\mu_u}{\delta t} M_u \left(U^{n+1} - U^n\right) + \tau_p \frac{\mu_p}{\delta t} M_{S,p} \left(P^{n+1} - P^n\right) + \theta \left(K_p P^{n+1} + \tau_p K_{S,u} U^{n+1}\right) \\
&\quad + (1-\theta)\left(K_p P^n + \tau_p K_{S,u} U^n\right) = 0.
\end{aligned}$$

We concentrate on one of the equations because both will be equivalent for the current analysis. The $j$th row of the system of equations is

$$\begin{aligned}
&\mu_p \frac{h}{6\delta t}\left(P_{j-1}^{n+1} + 4P_j^{n+1} + P_{j+1}^{n+1} - P_{j-1}^n - 4P_j^n - P_{j+1}^n\right) + \tau_u \frac{\mu_u}{2\delta t}\left(U_{j-1}^{n+1} - U_{j+1}^{n+1} - U_{j-1}^n + U_{j+1}^n\right) \\
&\quad + \theta\left(\frac{1}{2}\left(-U_{j-1}^{n+1} + U_{j+1}^{n+1}\right) + \tau_u \frac{1}{h}\left(-P_{j-1}^{n+1} + 2P_j^{n+1} - P_{j+1}^{n+1}\right)\right) \\
&\quad + (1-\theta)\left(\frac{1}{2}\left(-U_{j-1}^n + U_{j+1}^n\right) + \tau_u \frac{1}{h}\left(-P_{j-1}^n + 2P_j^n - P_{j+1}^n\right)\right) = 0,
\end{aligned}$$

and replacing $\left[P_j^n, U_j^n\right]$ from (44) we get

$$\begin{aligned}
&\mu_p \frac{h}{6\delta t}\left(\mathrm{e}^{\mathrm{i}(-kh-\omega_*\delta t)} + 4\mathrm{e}^{\mathrm{i}(-\omega_*\delta t)} + \mathrm{e}^{\mathrm{i}(kh-\omega_*\delta t)} - \mathrm{e}^{\mathrm{i}(-kh)} - 4 - \mathrm{e}^{\mathrm{i}(kh)}\right) \\
&\quad + \frac{1}{2\delta t}\tau_u \mu_p^{1/2}\mu_u^{1/2}\left(\mathrm{e}^{\mathrm{i}(-kh-\omega_*\delta t)} - \mathrm{e}^{\mathrm{i}(kh-\omega_*\delta t)} - \mathrm{e}^{\mathrm{i}(-kh)} + \mathrm{e}^{\mathrm{i}(kh)}\right) \\
&\quad + \theta\left(\frac{1}{2}\mu_p^{1/2}\mu_u^{-1/2}\left(-\mathrm{e}^{\mathrm{i}(-kh-\omega_*\delta t)} + \mathrm{e}^{\mathrm{i}(kh-\omega_*\delta t)}\right) + \frac{1}{h}\tau_u\left(-\mathrm{e}^{\mathrm{i}(-kh-\omega_*\delta t)} + 2\mathrm{e}^{\mathrm{i}(-\omega_*\delta t)} - \mathrm{e}^{\mathrm{i}(kh-\omega_*\delta t)}\right)\right) \\
&\quad + (1-\theta)\left(\frac{1}{2}\mu_p^{1/2}\mu_u^{-1/2}\left(-\mathrm{e}^{\mathrm{i}(-kh)} + \mathrm{e}^{\mathrm{i}(kh)}\right) + \frac{1}{h}\tau_u\left(-\mathrm{e}^{\mathrm{i}(-kh)} + 2 - \mathrm{e}^{\mathrm{i}(kh)}\right)\right) = 0.
\end{aligned}$$

Using the definition of $r$ from (45) we arrive at:

$$\frac{\omega_*}{\omega} = -\frac{1}{\mathrm{i}r(kh)}\log\left(\frac{-2 - \cos(kh) + 3\mathrm{i}C_\tau \sin(kh) + (1-\theta)(3\mathrm{i}r\sin(kh) + 6rC_\tau(1-\cos(kh)))}{3\mathrm{i}C_\tau \sin(kh) - 2 - \cos(kh) - 3\mathrm{i}r\theta\sin(kh) - 6r\theta C_\tau(1-\cos(kh))}\right).$$

Figs. 8–10 show the real and imaginary parts of the angular frequency ratio keeping two parameters fixed. It can be seen that $\theta = 0$ (forward Euler or explicit Euler scheme) is unconditionally unstable. This is similar to what happens with forward in time-centered in space finite differences (FTCS) applied to the pure advection equation in 1D.

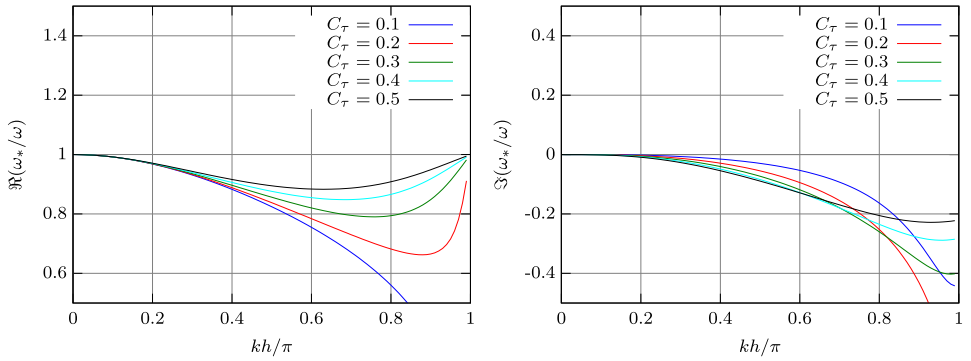


Fig. 9. ASGS + $\theta$ for $r = 1$ and $\theta = 0.5$.

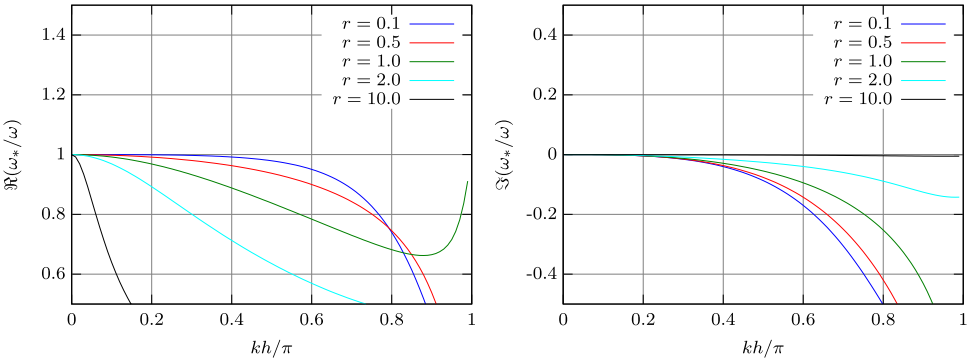


Fig. 10. ASGS + $\theta$ for $C_\tau = 0.2$ and $\theta = 0.5$.

Next, we consider the ASGS with the BDF2 time integration. The fully discrete problem is:

$$\frac{\mu_p}{2\delta t} M_p \left(3P^{n+2} - 4P^{n+1} + P^n\right) + \tau_u \frac{\mu_u}{2\delta t} M_{S,u} \left(3U^{n+2} - 4U^{n+1} + U^n\right) + K_u U^{n+2} + \tau_u K_{S,p} P^{n+2} = 0,$$
$$\frac{\mu_u}{2\delta t} M_u \left(3U^{n+2} - 4U^{n+1} + U^n\right) + \tau_p \frac{\mu_p}{2\delta t} M_{S,p} \left(3P^{n+2} - 4P^{n+1} + P^n\right) + K_p P^{n+2} + \tau_p K_{S,u} U^{n+2} = 0.$$

Following a similar procedure as before, we arrive at

$$\left(3\mathrm{e}^{-2\mathrm{i}\omega_*\delta t} - 4\mathrm{e}^{-\mathrm{i}\omega_*\delta t} + 1\right)((2 + \cos(kh)) - 3\mathrm{i}C_\tau\,(\sin(kh)))$$
$$+ \mathrm{e}^{-2\mathrm{i}\omega_*\delta t}\,(6\mathrm{i}r\,(\sin(kh)) + 12rC_\tau\,(1 - \cos(kh))) = 0.$$

Figs. 11 and 12 show the angular frequency ratio for the fully discrete problem. It can be seen that this combination of spatial and temporal discretization is stable.

Fig. 13 compares the fully discrete ASGS method with the two time integration schemes shown previously. It can be seen that the $\theta$ method performs better than BDF2 for small enough $kh$.

Next, we aim to analyze the properties of the OSS stabilized formulation. When using the $\theta$-method for the time integration, the fully discrete problem is:

$$\frac{\mu_p}{\delta t} M_p \left(P^{n+1} - P^n\right) + \tau_u \frac{\mu_u}{\delta t} M_{S,u} \left(U^{n+1} - U^n\right) - \tau_u M_{S,u} \widetilde{M}_u^{-1} \frac{\mu_u}{\delta t} M_u \left(U^{n+1} - U^n\right)$$
$$+ \theta \left(K_u U^{n+1} + \tau_u K_{S,p} P^{n+1} - \tau_u M_{S,u} \widetilde{M}_u^{-1} K_p P^{n+1}\right)$$
$$+ (1 - \theta) \left(K_u U^n + \tau_u K_{S,p} P^n - \tau_u M_{S,u} \widetilde{M}_u^{-1} K_p P^n\right) = 0,$$
$$\frac{\mu_u}{\delta t} M_u \left(U^{n+1} - U^n\right) + \tau_p \frac{\mu_p}{\delta t} M_{S,p} \left(P^{n+1} - P^n\right) - \tau_p M_{S,p} \widetilde{M}_p^{-1} \frac{\mu_p}{\delta t} M_p \left(P^{n+1} - P^n\right)$$

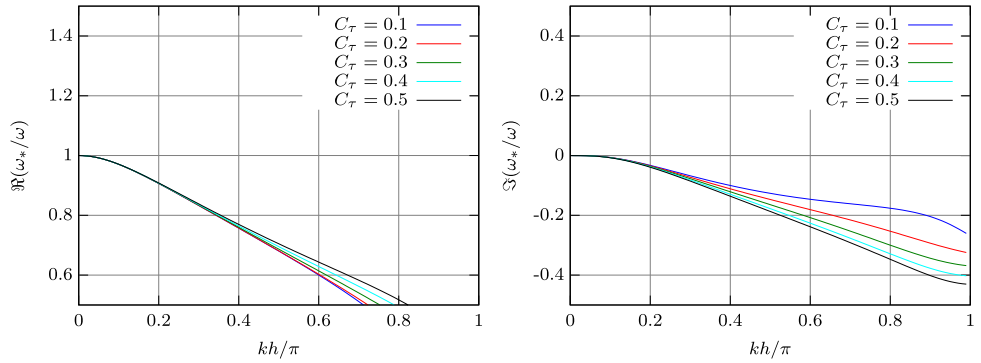


Fig. 11. ASGS + BDF2 for $r = 1$.

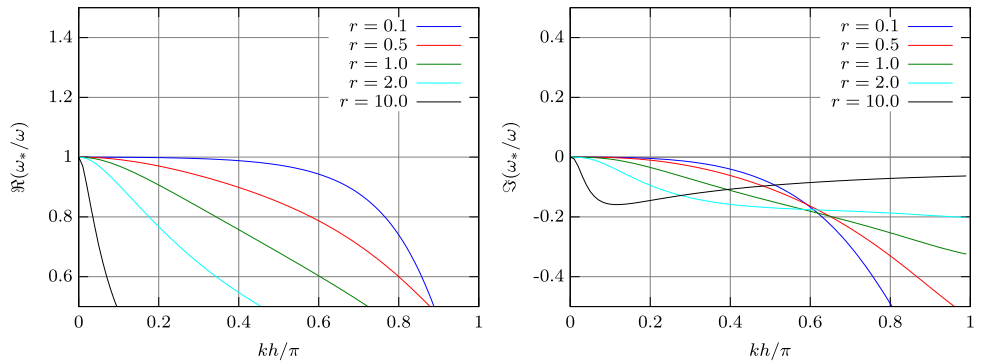


Fig. 12. ASGS + BDF2 for $C_\tau = 0.2$.

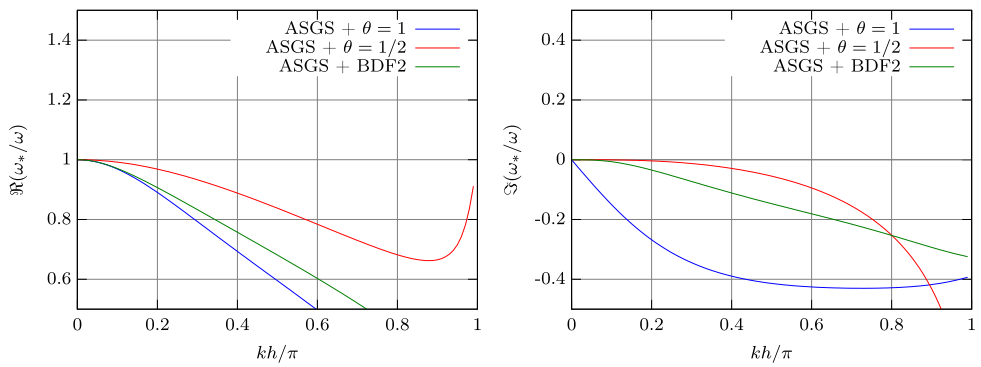


Fig. 13. Fully discrete ASGS with $C_\tau = 0.2$ and $r = 1$.

$$+\theta\left(K_p P^{n+1} + \tau_p K_{S,u} U^{n+1} - \tau_p M_{S,p} \widetilde{M}_p^{-1} K_u U^{n+1}\right)$$
$$+ (1-\theta)\left(K_p P^{n} + \tau_p K_{S,u} U^{n} - \tau_p M_{S,p} \widetilde{M}_p^{-1} K_u U^{n}\right) = 0.$$

Following a similar procedure as before we arrive at

$$\left(\mathrm{e}^{-\mathrm{i}\omega_* \delta t} - 1\right)\left(2\left(2 + \cos(kh)\right) + \mathrm{i}C_\tau\left(-2\sin(kh) + \sin(2kh)\right)\right)$$
$$+ \left(\theta \mathrm{e}^{-\mathrm{i}\omega_* \delta t} + 1 - \theta\right)\left(6\mathrm{i}r\left(\sin(kh)\right) + 3rC_\tau\left(3 - 4\cos(kh) + \cos(2kh)\right)\right) = 0.$$

Figs. 14–16 show the angular frequency ratio for this fully discretized problem.

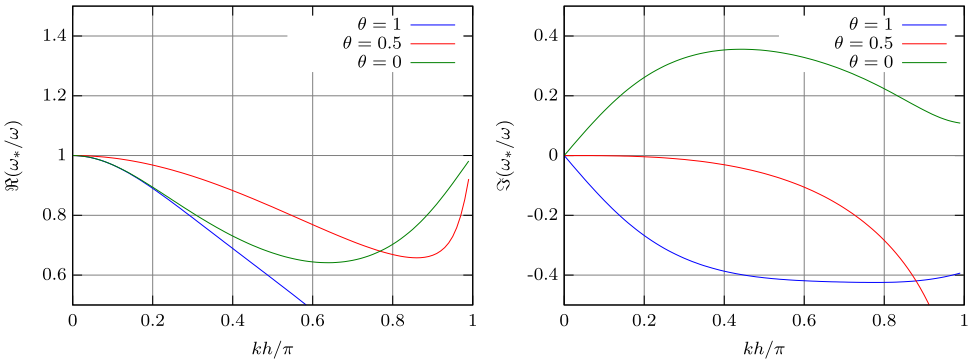


Fig. 14. OSS + $\theta$ for $r = 1$ and $C_\tau = 0.2$.

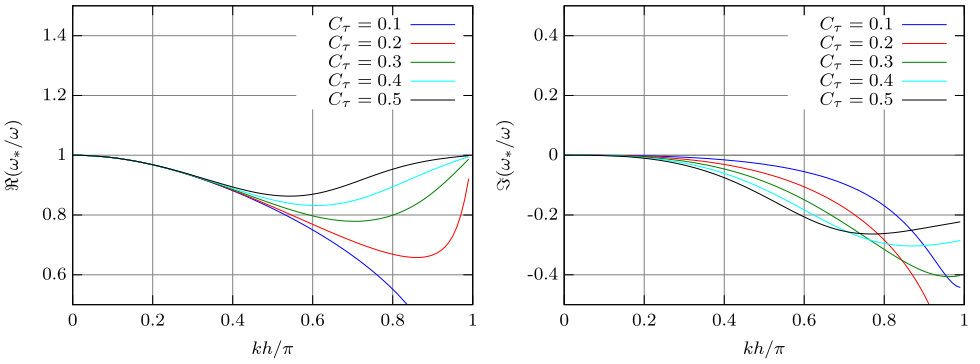


Fig. 15. OSS + $\theta$ for $r = 1$ and $\theta = 0.5$.

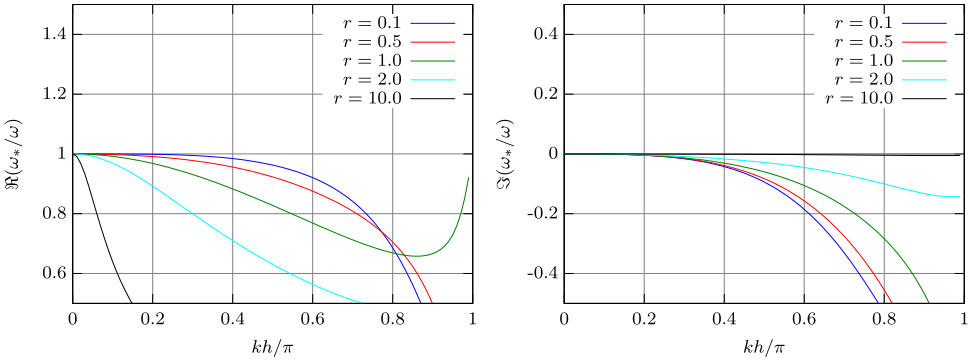


Fig. 16. OSS + $\theta$ for $C_\tau = 0.2$ and $\theta = 0.5$.

Next, we consider the OSS-BDF2 fully discrete problem:

$$\frac{\mu_p}{2\delta t} M_p \left(3P^{n+2} - 4P^{n+1} + P^n\right) + \tau_u \frac{\mu_u}{2\delta t} M_{S,u} \left(3U^{n+2} - 4U^{n+1} + U^n\right) + K_u U^{n+2} + \tau_u K_{S,p} P^{n+2}$$
$$- \tau_u M_{S,u} \widetilde{M}_u^{-1} \left(\frac{\mu_u}{2\delta t} M_u \left(3U^{n+2} - 4U^{n+1} + U^n\right) + K_p P^{n+2}\right) = 0,$$
$$\frac{\mu_u}{2\delta t} M_u \left(3U^{n+2} - 4U^{n+1} + U^n\right) + \tau_p \frac{\mu_p}{2\delta t} M_{S,p} \left(3P^{n+2} - 4P^{n+1} + P^n\right) + K_p P^{n+2} + \tau_p K_{S,u} U^{n+2}$$
$$- \tau_p M_{S,p} \widetilde{M}_p^{-1} \left(\frac{\mu_p}{2\delta t} M_p \left(3P^{n+2} - 4P^{n+1} + P^n\right) + K_u U^{n+2}\right) = 0.$$

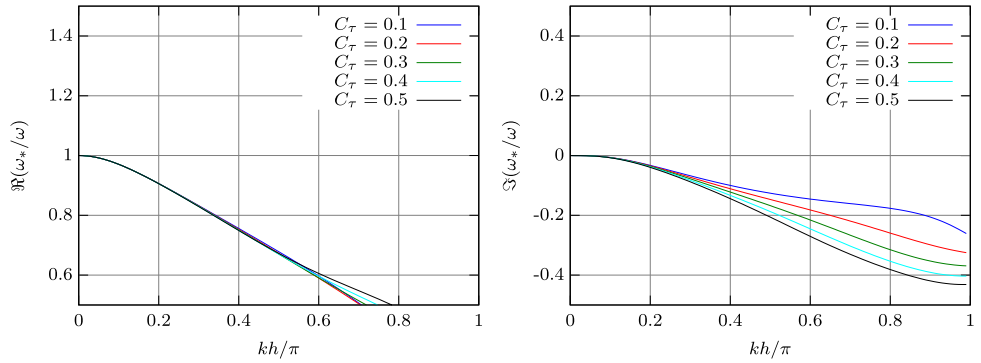


Fig. 17. OSS + BDF2 for $r = 1$.

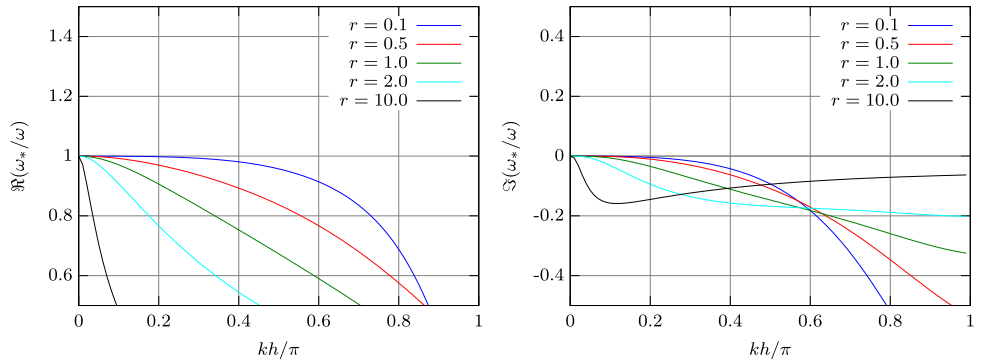


Fig. 18. OSS + BDF2 for $C_\tau = 0.2$.

Following a similar procedure as before we get

$$\left(3\mathrm{e}^{-2\mathrm{i}\omega_*\delta t} - 4\mathrm{e}^{-\mathrm{i}\omega_*\delta t} + 1\right)\left(2\left(2+\cos(kh)\right) + \mathrm{i}C_\tau\left(-2\sin(kh) + \sin(2kh)\right)\right)$$
$$+\,\mathrm{e}^{-2\mathrm{i}\omega_*\delta t}\left(12\mathrm{i}r\left(\sin(kh)\right) + 6rC_\tau\left(3 - 4\cos(kh) + \cos(2kh)\right)\right) = 0.$$

Figs. 17 and 18 show the real and imaginary parts of the angular frequency ratio.

The plots comparing time marching schemes for the OSS method are very similar to the ones for ASGS and are not shown for succinctness. The fully discrete ASGS and OSS methods perform similarly according to this analysis, so we do not show a side by side comparison of both methods.

## 5. Numerical results

In this section we present two sets of numerical results. First, convergence tests are presented and compared with the predicted convergence rates obtained from convergence analysis. Then, numerical solutions of a wave propagation problem are compared in order to see the differences of the fully discrete methods.

### 5.1. Convergence tests

Let us consider a two dimensional transient problem with analytical solution to investigate the convergence properties of the stabilized FE formulations proposed. The spatial domain is the unit square $(0, 1) \times (0, 1)$ and the temporal domain is $(0, 1)$. The forcing terms $\left[f_p, \boldsymbol{f}_u\right]$ are chosen such that the exact solution is $p = \sin(\pi x)\sin(\pi y)\cos\left(\frac{\pi}{3}t\right)$ and $\boldsymbol{u} = [p, p]$ with $\mu_p = \mu_u = 1$. On the boundary we prescribe $p = 0$ ($\Gamma = \Gamma_p$). The initial condition is taken as the exact solution at $t = 0$. Various mesh sizes and time step sizes have been used to generate the results. We have used isotropic bilinear ($Q1$) and biquadratic ($Q2$) meshes of sizes $h = 0.05, 0.025, 0.01, 0.005$ and $0.002$. The

Table 9
Experimental $\delta t$ convergence rates for ASGS-BE method using $Q1/Q1$ spatial interpolation.

| Variational form | I | | II | | III | | I | |
|---|---|---|---|---|---|---|---|---|
| $\delta t$ vs. $h$ | $\delta t \sim 0.5h$ | | | | | | $\delta t \sim 4.5h^{1.5}$ | |
| | Num | Min | Num | Min | Num | Min | Num | Min |
| $\|p^n - p_h^n\|_{\ell^\infty(L^2)}$ | 1.00 | 1 | 1.00 | 1 | 1.01 | 1 | 1.00 | 1 |
| $\|\boldsymbol{u}^n - \boldsymbol{u}_h^n\|_{\ell^\infty(L^2)}$ | 1.02 | 1 | 1.02 | 1 | 1.02 | 1 | 1.01 | 1 |
| $\|\nabla(p^n - p_h^n)\|_{\ell^2(L^2)}$ | 1.00 | 0.5 | 1.00 | 0 | 1.00 | 1 | 0.66 | 2/3 |
| $\|\nabla\cdot(\boldsymbol{u}^n - \boldsymbol{u}_h^n)\|_{\ell^2(L^2)}$ | 1.00 | 0.5 | 1.00 | 1 | 1.00 | 0 | 0.66 | 2/3 |

Table 10
Experimental $\delta t$ convergence rates for OSS-BE method using $Q1/Q1$ spatial interpolation.

| Variational form | I | | II | | III | | I | |
|---|---|---|---|---|---|---|---|---|
| $\delta t$ vs. $h$ | $\delta t \sim 0.5h$ | | | | | | $\delta t \sim 4.5h^{1.5}$ | |
| | Num | Min | Num | Min | Num | Min | Num | Min |
| $\|p^n - p_h^n\|_{\ell^\infty(L^2)}$ | 1.00 | 1 | 1.00 | 1 | 1.01 | 1 | 1.00 | 1 |
| $\|\boldsymbol{u}^n - \boldsymbol{u}_h^n\|_{\ell^\infty(L^2)}$ | 1.02 | 1 | 1.02 | 1 | 1.02 | 1 | 1.01 | 1 |
| $\|\nabla(p^n - p_h^n)\|_{\ell^2(L^2)}$ | 1.00 | 0.5 | 1.00 | 0 | 1.00 | 1 | 0.66 | 2/3 |
| $\|\nabla\cdot(\boldsymbol{u}^n - \boldsymbol{u}_h^n)\|_{\ell^2(L^2)}$ | 1.00 | 0.5 | 1.00 | 1 | 1.00 | 0 | 0.66 | 2/3 |

Table 11
Experimental $\delta t$ convergence rates for ASGS-BE method using $Q2/Q2$ spatial interpolation.

| Variational form | I | | II | | III | | I | | II | | III | |
|---|---|---|---|---|---|---|---|---|---|---|---|---|
| $\delta t$ vs. $h$ | $\delta t \sim 0.5h$ | | | | | | $\delta t \sim 894h^{2.5}$ | | $\delta t \sim 40h^2$ | | $\delta t \sim 40h^2$ | |
| | Num | Min | Num | Min | Num | Min | Num | Min | Num | Min | Num | Min |
| $\|p^n - p_h^n\|_{\ell^\infty(L^2)}$ | 0.98 | 1 | 0.98 | 1 | 0.98 | 1 | 0.99 | 1 | 0.99 | 1 | 0.99 | 1 |
| $\|\boldsymbol{u}^n - \boldsymbol{u}_h^n\|_{\ell^\infty(L^2)}$ | 0.99 | 1 | 0.99 | 1 | 0.99 | 1 | 1.00 | 1 | 1.00 | 1 | 1.00 | 1 |
| $\|\nabla(p^n - p_h^n)\|_{\ell^2(L^2)}$ | 0.99 | 0.5 | 0.99 | 0 | 0.99 | 1 | 0.98 | 4/5 | 0.50 | 0.5 | 1.00 | 1 |
| $\|\nabla\cdot(\boldsymbol{u}^n - \boldsymbol{u}_h^n)\|_{\ell^2(L^2)}$ | 0.99 | 0.5 | 0.99 | 1 | 0.99 | 0 | 0.99 | 4/5 | 1.00 | 1 | 0.50 | 0.5 |

stabilization algorithmic constant $C_\tau$ has been taken as 0.05 for $Q1$ elements and 0.4 for $Q2$ elements. The length scale of the problem has been taken as $L_0 = \sqrt[d]{\text{meas}(\Omega)} = 1$.

In Tables 9–20 we show the convergence rates with respect to the time step size $\delta t$ for various stabilization methods (ASGS and OSS), time integrators (BE/CN/BDF2) and spatial interpolations ($Q1$ and $Q2$). The numerical experiments have been carried out modifying the time step size and the mesh size at the same time. The relationship $(\delta t, h)$ is shown in each table for each variational form with the respective proportionality constant and power, $\delta t \sim C_s h^s$. The power constant $s$ has been chosen in two ways, first as $s = 1$ for all the variational forms and, secondly, it has been chosen such that the best convergence is achieved for equal interpolation of the unknowns ($k = l$); see Tables 9–20. It is observed that in all cases the numerical rate of convergence obtained (Num) is greater than or equal to the minimum one predicted by the convergence analysis (Min). Note that in some cases a clear superconvergence phenomenon is observed.

### 5.2. Numerical comparison

In Section 4 we analyzed dispersion and dissipation analytically through Fourier techniques. We present now a simple test to verify experimentally the predictions of the Fourier analysis. Let us consider a 1D problem in $\Omega = (0, L) = (0, 1)$ and $\Upsilon = (0, 0.8)$, and let us solve the mixed wave equation with $\mu_p = 1$, $\mu_u = 1$, zero initial conditions and boundary conditions $p(0, t) = \sin(\omega t)$ and $p(L, t) = 0$. We compare the solutions obtained with the fully discrete methods at $t = 0.6$.

Table 12
Experimental $\delta t$ convergence rates for OSS-BE method using $Q2/Q2$ spatial interpolation.

| Variational form | I | | II | | III | | I | | II | | III | |
|---|---|---|---|---|---|---|---|---|---|---|---|---|
| $\delta t$ vs. $h$ | $\delta t \sim 0.5h$ | | | | | | $\delta t \sim 894h^{2.5}$ | | $\delta t \sim 40h^2$ | | $\delta t \sim 40h^2$ | |
| | Num | Min | Num | Min | Num | Min | Num | Min | Num | Min | Num | Min |
| $\|p^n - p_h^n\|_{\ell^\infty(L^2)}$ | 0.98 | 1 | 0.98 | 1 | 0.98 | 1 | 0.99 | 1 | 0.99 | 1 | 0.99 | 1 |
| $\|\boldsymbol{u}^n - \boldsymbol{u}_h^n\|_{\ell^\infty(L^2)}$ | 0.99 | 1 | 0.99 | 1 | 0.99 | 1 | 1.00 | 1 | 1.00 | 1 | 1.00 | 1 |
| $\|\nabla(p^n - p_h^n)\|_{\ell^2(L^2)}$ | 0.99 | 0.5 | 1.02 | 0 | 0.99 | 1 | 0.98 | 4/5 | 0.51 | 0.5 | 1.00 | 1 |
| $\|\nabla\cdot(\boldsymbol{u}^n - \boldsymbol{u}_h^n)\|_{\ell^2(L^2)}$ | 0.99 | 0.5 | 0.99 | 1 | 1.03 | 0 | 0.99 | 4/5 | 0.99 | 1 | 0.52 | 0.5 |

Table 13
Experimental $\delta t$ convergence rates for ASGS-CN method using $Q1/Q1$ spatial interpolation.

| Variational form | I | | II | | III | | I | | II | | III | |
|---|---|---|---|---|---|---|---|---|---|---|---|---|
| $\delta t$ vs. $h$ | $\delta t \sim 0.5h$ | | | | | | $\delta t \sim 0.2h^{0.75}$ | | $\delta t \sim 0.1h^{0.5}$ | | $\delta t \sim 0.1h^{0.5}$ | |
| | Num | Min | Num | Min | Num | Min | Num | Min | Num | Min | Num | Min |
| $\|p^n - p_h^n\|_{\ell^\infty(L^2)}$ | 2.00 | 1.5 | 2.00 | 1 | 2.00 | 1 | 2.60 | 2 | 3.38 | 2 | 3.39 | 2 |
| $\|\boldsymbol{u}^n - \boldsymbol{u}_h^n\|_{\ell^\infty(L^2)}$ | 2.00 | 1.5 | 2.00 | 1 | 2.00 | 1 | 2.64 | 2 | 3.72 | 2 | 3.72 | 2 |
| $\|\nabla(p^n - p_h^n)\|_{\ell^2(L^2)}$ | 1.00 | 1 | 1.00 | 0 | 1.00 | 1 | 1.33 | 4/3 | 1.99 | 0 | 1.99 | 2 |
| $\|\nabla\cdot(\boldsymbol{u}^n - \boldsymbol{u}_h^n)\|_{\ell^2(L^2)}$ | 1.00 | 1 | 1.00 | 1 | 1.00 | 0 | 1.33 | 4/3 | 1.99 | 2 | 1.99 | 0 |

Table 14
Experimental $\delta t$ convergence rates for OSS-CN method using $Q1/Q1$ spatial interpolation.

| Variational form | I | | II | | III | | I | | II | | III | |
|---|---|---|---|---|---|---|---|---|---|---|---|---|
| $\delta t$ vs. $h$ | $\delta t \sim 0.5h$ | | | | | | $\delta t \sim 0.2h^{0.75}$ | | $\delta t \sim 0.1h^{0.5}$ | | $\delta t \sim 0.1h^{0.5}$ | |
| | Num | Min | Num | Min | Num | Min | Num | Min | Num | Min | Num | Min |
| $\|p^n - p_h^n\|_{\ell^\infty(L^2)}$ | 2.00 | 1.5 | 2.00 | 1 | 2.00 | 1 | 2.60 | 2 | 3.38 | 2 | 3.39 | 2 |
| $\|\boldsymbol{u}^n - \boldsymbol{u}_h^n\|_{\ell^\infty(L^2)}$ | 2.00 | 1.5 | 2.00 | 1 | 2.00 | 1 | 2.64 | 2 | 3.72 | 2 | 3.72 | 2 |
| $\|\nabla(p^n - p_h^n)\|_{\ell^2(L^2)}$ | 1.00 | 1 | 1.00 | 0 | 1.00 | 1 | 1.33 | 4/3 | 1.99 | 0 | 1.99 | 2 |
| $\|\nabla\cdot(\boldsymbol{u}^n - \boldsymbol{u}_h^n)\|_{\ell^2(L^2)}$ | 1.00 | 1 | 1.00 | 1 | 1.00 | 0 | 1.33 | 4/3 | 1.99 | 2 | 1.99 | 0 |

Table 15
Experimental $\delta t$ convergence rates for ASGS-CN method using $Q2/Q2$ spatial interpolation.

| Variational form | I | | II | | III | | I | |
|---|---|---|---|---|---|---|---|---|
| $\delta t$ vs. $h$ | $\delta t \sim 0.5h$ | | | | | | $\delta t \sim 2h^{1.25}$ | |
| | Num | Min | Num | Min | Num | Min | Num | Min |
| $\|p^n - p_h^n\|_{\ell^\infty(L^2)}$ | 2.01 | 2 | 2.00 | 2 | 2.00 | 2 | 2.00 | 2 |
| $\|\boldsymbol{u}^n - \boldsymbol{u}_h^n\|_{\ell^\infty(L^2)}$ | 2.26 | 2 | 2.00 | 2 | 2.00 | 2 | 2.13 | 2 |
| $\|\nabla(p^n - p_h^n)\|_{\ell^2(L^2)}$ | 1.99 | 1.5 | 1.00 | 1 | 2.00 | 2 | 1.60 | 1.6 |
| $\|\nabla\cdot(\boldsymbol{u}^n - \boldsymbol{u}_h^n)\|_{\ell^2(L^2)}$ | 1.99 | 1.5 | 2.00 | 2 | 1.00 | 1 | 1.60 | 1.6 |

For $\omega = 10\pi$ a quite coarse pair of mesh and time step sizes is $(h, \delta t) = (0.05, 0.05)$. This allows us to see dispersion and dissipation in the numerical solution when compared with the exact solution $\sin(\omega t - kx)(1 - H(x - ct))$, where $H$ is the Heaviside step function. The algorithmic constant is taken as $C_\tau = 0.1$ and the elements used are P1.

Fig. 19 shows the numerical solutions obtained with ASGS and three time marching schemes. CN is the least dissipative while BE is the most dissipative and BDF2 is somewhere in the middle. These numerical results are in agreement with the previous Fourier analysis. OSS behaves similarly and we do not show those results. Figs. 20–22

Table 16
Experimental $\delta t$ convergence rates for OSS-CN method using $Q2/Q2$ spatial interpolation.

| Variational form | I | | II | | III | | I | |
|---|---|---|---|---|---|---|---|---|
| $\delta t$ vs. $h$ | $\delta t \sim 0.5h$ | | | | | | $\delta t \sim 2h^{1.25}$ | |
| | Num | Min | Num | Min | Num | Min | Num | Min |
| $\left\|p^n - p_h^n\right\|_{\ell^\infty(L^2)}$ | 2.01 | 2 | 1.99 | 2 | 2.00 | 2 | 2.00 | 2 |
| $\left\|\boldsymbol{u}^n - \boldsymbol{u}_h^n\right\|_{\ell^\infty(L^2)}$ | 2.04 | 2 | 1.99 | 2 | 2.03 | 2 | 2.00 | 2 |
| $\left\|\nabla(p^n - p_h^n)\right\|_{\ell^2(L^2)}$ | 2.00 | 1.5 | 1.00 | 1 | 2.00 | 2 | 1.60 | 1.6 |
| $\left\|\nabla\cdot(\boldsymbol{u}^n - \boldsymbol{u}_h^n)\right\|_{\ell^2(L^2)}$ | 2.02 | 1.5 | 1.98 | 2 | 1.02 | 1 | 1.62 | 1.6 |

Table 17
Experimental $\delta t$ convergence rates for ASGS-BDF2 method using $Q1/Q1$ spatial interpolation.

| Variational form | I | | II | | III | | I | | II | | III | |
|---|---|---|---|---|---|---|---|---|---|---|---|---|
| $\delta t$ vs. $h$ | $\delta t \sim 0.5h$ | | | | | | $\delta t \sim 0.2h^{0.75}$ | | $\delta t \sim 0.1h^{0.5}$ | | $\delta t \sim 0.1h^{0.5}$ | |
| | Num | Min | Num | Min | Num | Min | Num | Min | Num | Min | Num | Min |
| $\left\|p^n - p_h^n\right\|_{\ell^\infty(L^2)}$ | 2.00 | 1.5 | 2.00 | 1 | 2.00 | 1 | 2.66 | 2 | 3.93 | 2 | 3.93 | 2 |
| $\left\|\boldsymbol{u}^n - \boldsymbol{u}_h^n\right\|_{\ell^\infty(L^2)}$ | 2.00 | 1.5 | 2.00 | 1 | 2.00 | 1 | 2.67 | 2 | 4.04 | 2 | 4.04 | 2 |
| $\left\|\nabla(p^n - p_h^n)\right\|_{\ell^2(L^2)}$ | 1.00 | 1 | 1.00 | 0 | 1.00 | 1 | 1.32 | 4/3 | 1.99 | 0 | 1.99 | 2 |
| $\left\|\nabla\cdot(\boldsymbol{u}^n - \boldsymbol{u}_h^n)\right\|_{\ell^2(L^2)}$ | 1.00 | 1 | 1.00 | 1 | 1.00 | 0 | 1.32 | 4/3 | 1.99 | 2 | 1.99 | 0 |

Table 18
Experimental $\delta t$ convergence rates for OSS-BDF2 method using $Q1/Q1$ spatial interpolation.

| Variational form | I | | II | | III | | I | | II | | III | |
|---|---|---|---|---|---|---|---|---|---|---|---|---|
| $\delta t$ vs. $h$ | $\delta t \sim 0.5h$ | | | | | | $\delta t \sim 0.2h^{0.75}$ | | $\delta t \sim 0.1h^{0.5}$ | | $\delta t \sim 0.1h^{0.5}$ | |
| | Num | Min | Num | Min | Num | Min | Num | Min | Num | Min | Num | Min |
| $\left\|p^n - p_h^n\right\|_{\ell^\infty(L^2)}$ | 2.00 | 1.5 | 2.00 | 1 | 2.00 | 1 | 2.66 | 2 | 3.93 | 2 | 3.93 | 2 |
| $\left\|\boldsymbol{u}^n - \boldsymbol{u}_h^n\right\|_{\ell^\infty(L^2)}$ | 2.00 | 1.5 | 2.00 | 1 | 2.00 | 1 | 2.67 | 2 | 4.04 | 2 | 4.04 | 2 |
| $\left\|\nabla(p^n - p_h^n)\right\|_{\ell^2(L^2)}$ | 1.00 | 1 | 1.00 | 0 | 1.00 | 1 | 1.32 | 4/3 | 1.99 | 0 | 1.99 | 2 |
| $\left\|\nabla\cdot(\boldsymbol{u}^n - \boldsymbol{u}_h^n)\right\|_{\ell^2(L^2)}$ | 1.00 | 1 | 1.00 | 1 | 1.00 | 0 | 1.32 | 4/3 | 1.99 | 2 | 1.99 | 0 |

Table 19
Experimental $\delta t$ convergence rates for ASGS-BDF2 method using $Q2/Q2$ spatial interpolation.

| Variational form | I | | II | | III | | I | |
|---|---|---|---|---|---|---|---|---|
| $\delta t$ vs. $h$ | $\delta t \sim 0.5h$ | | | | | | $\delta t \sim 2h^{1.25}$ | |
| | Num | Min | Num | Min | Num | Min | Num | Min |
| $\left\|p^n - p_h^n\right\|_{\ell^\infty(L^2)}$ | 2.17 | 2 | 2.00 | 2 | 2.13 | 2 | 2.41 | 2 |
| $\left\|\boldsymbol{u}^n - \boldsymbol{u}_h^n\right\|_{\ell^\infty(L^2)}$ | 2.19 | 2 | 2.00 | 2 | 2.00 | 2 | 2.34 | 2 |
| $\left\|\nabla(p^n - p_h^n)\right\|_{\ell^2(L^2)}$ | 1.99 | 1.5 | 1.00 | 1 | 2.00 | 2 | 1.59 | 1.6 |
| $\left\|\nabla\cdot(\boldsymbol{u}^n - \boldsymbol{u}_h^n)\right\|_{\ell^2(L^2)}$ | 1.99 | 1.5 | 2.00 | 2 | 1.00 | 1 | 1.59 | 1.6 |

compare the ASGS method with the OSS method for the same time integration scheme, showing a very similar numerical behavior.

## 6. Conclusions

In this work we have presented fully discrete methods arising from the combination of spatial discretization methods, namely stabilized FE methods, and temporal discretization methods (backward Euler, Crank–Nicolson and

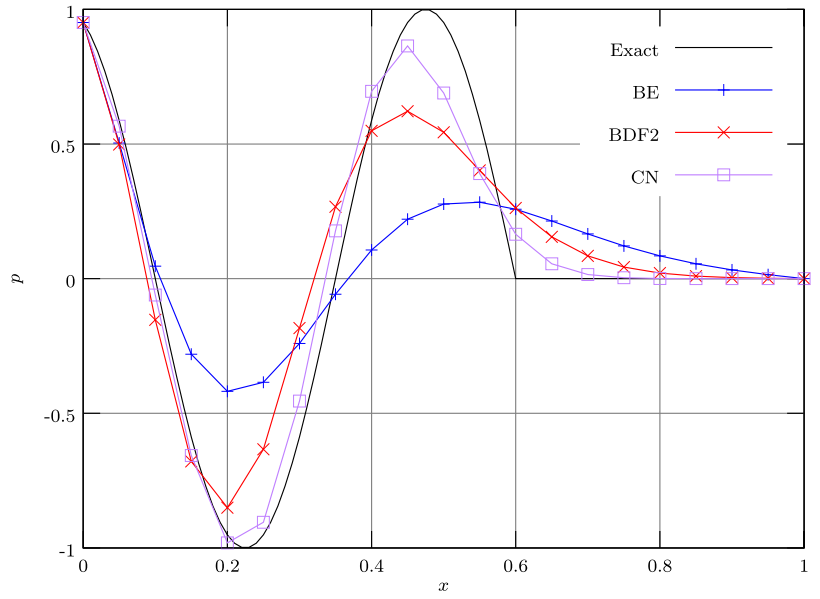


Fig. 19. Numerical solution using the ASGS formulation and different time marching schemes.

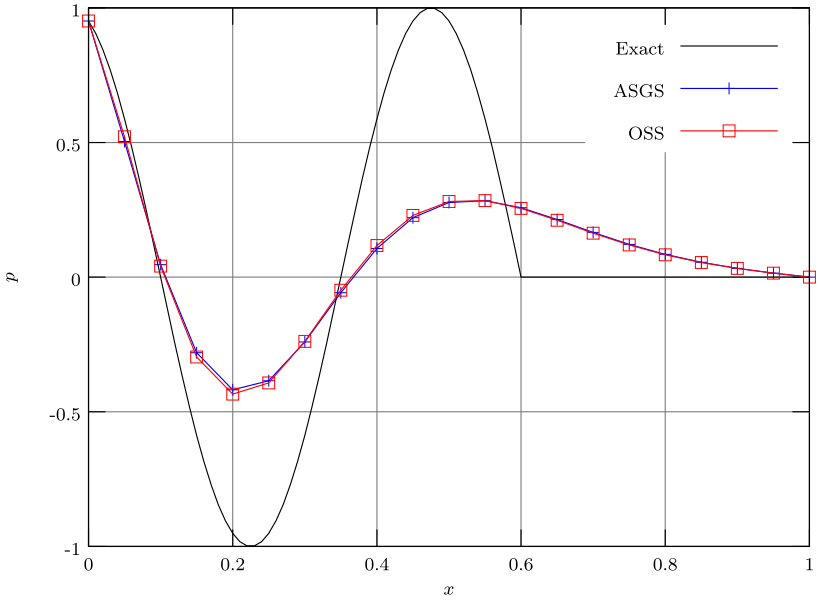


Fig. 20. Comparison of ASGS and OSS using BE as time integration.

2nd order backward differentiation formula) for the mixed wave equation in three different variational forms. The stabilization parameters have been designed such that they mimic the continuous setting.

Stability and convergence has been proved for all combinations of space discretization and time discretization. Stability, dispersion and dissipation of the fully discrete methods in 1D for equal interpolation of $[p, \boldsymbol{u}]$ have been analyzed using Fourier techniques. According to this analysis, CN performs better than BE and BDF2. Additionally, ASGS and OSS perform similarly.

Numerical convergence tests have been performed and the results obtained in the numerical experiments are in agreement with the theoretical predictions. Additionally, the fully discrete methods have been compared qualitatively.

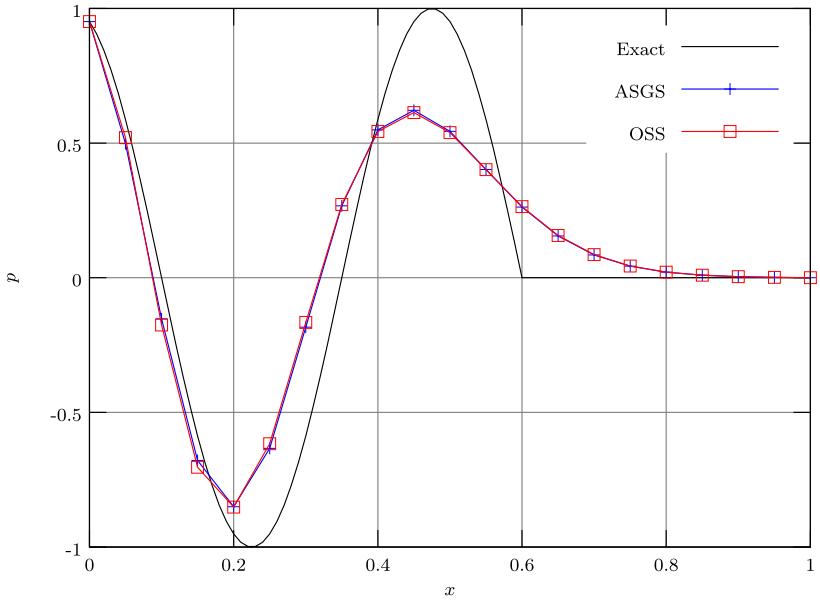


Fig. 21. Comparison of ASGS and OSS using BDF2 as time integration.

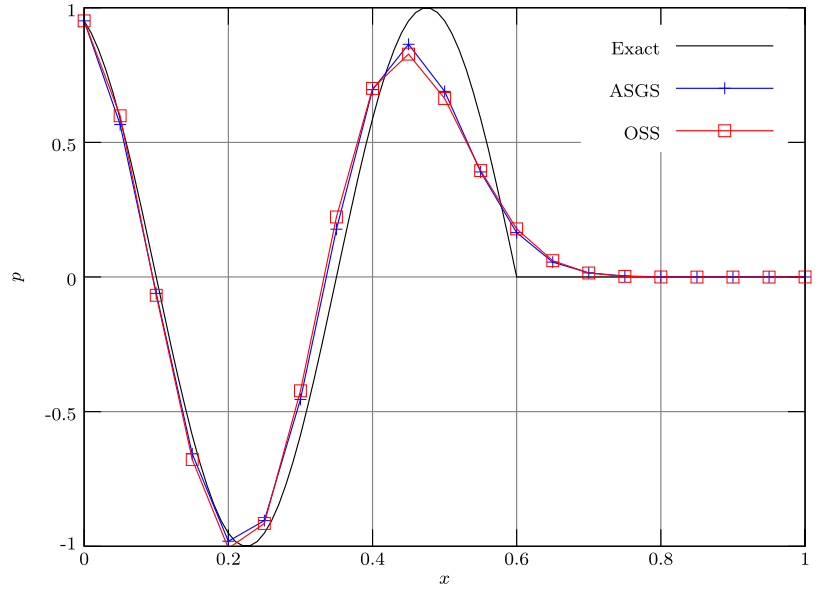


Fig. 22. Comparison of ASGS and OSS using CN as time integration.

Table 20
Experimental $\delta t$ convergence rates for OSS-BDF2 method using $Q2/Q2$ spatial interpolation.

| Variational form | I | | II | | III | | I | |
|---|---|---|---|---|---|---|---|---|
| $\delta t$ vs. $h$ | $\delta t \sim 0.5h$ | | | | | | $\delta t \sim 2h^{1.25}$ | |
| | Num | Min | Num | Min | Num | Min | Num | Min |
| $\|p^n - p_h^n\|_{\ell^\infty(L^2)}$ | 2.18 | 2 | 2.02 | 2 | 2.14 | 2 | 2.42 | 2 |
| $\|\boldsymbol{u}^n - \boldsymbol{u}_h^n\|_{\ell^\infty(L^2)}$ | 2.03 | 2 | 2.00 | 2 | 2.03 | 2 | 2.24 | 2 |
| $\|\nabla(p^n - p_h^n)\|_{\ell^2(L^2)}$ | 2.00 | 1.5 | 1.01 | 1 | 2.00 | 2 | 1.60 | 1.6 |
| $\|\nabla \cdot (\boldsymbol{u}^n - \boldsymbol{u}_h^n)\|_{\ell^2(L^2)}$ | 2.02 | 1.5 | 2.00 | 2 | 1.03 | 1 | 1.64 | 1.6 |

This comparison shows the differences in dispersion and dissipation of the methods and is in agreement with the Fourier analysis.

## Acknowledgments

The work of the first author was funded by the Ministerio de Educación, Cultura y Deporte, Programa de Formación del Profesorado Universitario (FPU), in Spain, with grant AP2010-0563, the work of the second author by the FP7 Grant No. 308874 (project Eunison) and the ICREA Acadèmia Program from the Catalan Government, and the work of the third author was funded by the European Research Council under the FP7 Programme Ideas through the Starting Grant No. 258443- COMFUS: Computational Methods for Fusion Technology.

## References

[1] J. Berland, C. Bogey, C. Bailly, Low-dissipation and low-dispersion fourth-order Runge–Kutta algorithm, Comput. & Fluids 35 (2006) 1459–1463.
[2] K. Tselios, T. Simos, Runge–Kutta methods with minimal dispersion and dissipation for problems arising from computational acoustics, J. Comput. Appl. Math. 175 (2005) 173–181.
[3] H. Xu, P. Sagaut, Optimal low-dispersion low-dissipation LBM schemes for computational aeroacoustics, J. Comput. Phys. 230 (2011) 5353–5382.
[4] J. Li, Z. Yang, The von neumann analysis and modified equation approach for finite difference schemes, Appl. Math. Comput. 225 (2013) 610–621.
[5] G. Scovazzi, J.N. Shadid, E. Love, W.J. Rider, A conservative nodal variational multiscale method for Lagrangian shock hydrodynamics, Comput. Methods Appl. Mech. Engrg. 199 (2010) 3059–3100.
[6] J. Nordström, Conservative finite difference formulations, variable coefficients, energy estimates and artificial dissipation, J. Sci. Comput. 29 (2006) 375–404.
[7] P. Joly, J. Rodríguez, Optimized higher order time discretization of second order hyperbolic problems: Construction and numerical study, J. Comput. Appl. Math. 234 (2010) 1953–1961.
[8] Y. Sun, P. Tse, Symplectic and multisymplectic numerical methods for Maxwell's equations, J. Comput. Phys. 230 (2011) 2076–2094.
[9] R. Codina, Finite element approximation of the hyperbolic wave equation in mixed form, Comput. Methods Appl. Mech. Engrg. 197 (2008) 1305–1322.
[10] S. Badia, R. Codina, H. Espinoza, Stability, convergence, and accuracy of stabilized finite element methods for the wave equation in mixed form, SIAM J. Numer. Anal. 52 (2014) 1729–1752.
[11] H. Espinoza, R. Codina, S. Badia, A Sommerfeld non-reflecting boundary condition for the wave equation in mixed form, Comput. Methods Appl. Mech. Engrg. 276 (2014) 122–148.
[12] S. Badia, R. Codina, Analysis of a stabilized finite element approximation of the transient convection–diffusion equation using an ALE framework, SIAM J. Numer. Anal. 44 (2006) 2159–2197.
[13] E. Burman, M.A. Fernández, Galerkin finite element methods with symmetric pressure stabilization for the transient Stokes equations: Stability and convergence analysis, SIAM J. Numer. Anal. 47 (2008) 409–439.
[14] E. Burman, Consistent SUPG-method for transient transport problems: Stability and convergence, Comput. Methods Appl. Mech. Engrg. 199 (2010) 1114–1123.
[15] T. Hughes, L. Franca, G. Hulbert, A new finite element formulation for computational fluid dynamics: VIII. The Galerkin/least-squares method for advective-diffusive equations, Comput. Methods Appl. Mech. Engrg. 73 (1989) 173–189.
[16] J. Lopez-Marcos, Crank-Nicolson method, in: Encyclopedia of Mathematics, Springer, 2012, p. p. 1.
[17] G. Noh, S. Ham, K.-J. Bathe, Performance of an implicit time integration scheme in the analysis of wave propagations, Comput. Struct. 123 (2013) 93–105.
[18] A. Idesman, H. Samajder, E. Aulisa, P. Seshaiyer, Benchmark problems for wave propagation in elastic materials, Comput. Mech. 43 (2009) 797–814.
[19] R. Codina, Analysis of a stabilized finite element approximation of the Oseen equations using orthogonal subscales, Appl. Numer. Math. 58 (2008) 264–283.
[20] T.J. Hughes, Multiscale phenomena: Green's functions, the Dirichlet-to-Neumann formulation, subgrid scale models, bubbles and the origins of stabilized methods, Comput. Methods Appl. Mech. Engrg. 127 (1995) 387–401.
[21] T.J. Hughes, G.R. Feijoo, L. Mazzei, J.-B. Quincy, The variational multiscale method-A paradigm for computational mechanics, Comput. Methods Appl. Mech. Engrg. 166 (1998) 3–24.
[22] R. Codina, Stabilization of incompressibility and convection through orthogonal sub-scales in finite element methods, Comput. Methods Appl. Mech. Engrg. 190 (2000) 1579–1599.
[23] R. Codina, Stabilized finite element approximation of transient incompressible flows using orthogonal subscales, Comput. Methods Appl. Mech. Engrg. 191 (2002) 4295–4321.
[24] R. Codina, J. Principe, O. Guasch, S. Badia, Time dependent subscales in the stabilized finite element approximation of incompressible flow problems, Comput. Methods Appl. Mech. Engrg. 196 (2007) 2413–2430.
[25] S. Badia, R. Codina, On a multiscale approach to the transient Stokes problem: Dynamic subscales and anisotropic space–time discretization, Appl. Math. Comput. 207 (2009) 415–433.

[26] S. Badia, R. Codina, Unified stabilized finite element formulations for the Stokes and the Darcy problems, SIAM J. Numer. Anal. 47 (2009) 1971–2000.
[27] A.-S. Bonnet-BenDhia, P. Ciarlet, C. Zwölf, Time harmonic wave diffraction problems in materials with sign-shifting coefficients, J. Comput. Appl. Math. 234 (2010) 1912–1919.
[28] A.-S. Bonnet-BenDhia, L. Chesnel, H. Haddar, On the use of T-coercivity to study the interior transmission eigenvalue problem, C. R. Math. Acad. Sci. Paris 349 (2011) 647–651.
[29] L. Chesnel, P. Ciarlet, T-coercivity and continuous galerkin methods: application to transmission problems with sign changing coefficients, Numer. Math. 124 (2013) 1–29.
[30] A.-S. Bonnet-BenDhia, L. Chesnel, P. Ciarlet, T-coercivity for the Maxwell problem with sign-changing coefficients, Comm. Partial Differential Equations 39 (2014) 1007–1031.
[31] J.-L. Guermond, R. Pasquetti, A correction technique for the dispersive effects of mass lumping for transport problems, Comput. Methods Appl. Mech. Engrg. 253 (2013) 186–198.